Article

SOURCE DATA TRANSPARENT PROCESS

THE EMBO JOURNAL

The mRNA decay factor PAT1 functions in a pathway including MAP kinase 4 and immune receptor SUMM2

Milena Edna Roux[1,†], Magnus Wohlfahrt Rasmussen[1,†], Kristoffer Palma[2], Signe Lolle[1], Àngels Mateu Regué[1], Gerit Bethke[3], Jane Glazebrook[3], Weiping Zhang[4], Leslie Sieburth[4], Martin R Larsen[5], John Mundy[1] & Morten Petersen[1,*]

Abstract

Multi-layered defense responses are activated in plants upon recognition of invading pathogens. Transmembrane receptors recognize conserved pathogen-associated molecular patterns (PAMPs) and activate MAP kinase cascades, which regulate changes in gene expression to produce appropriate immune responses. For example, *Arabidopsis* MAP kinase 4 (MPK4) regulates the expression of a subset of defense genes via at least one WRKY transcription factor. We report here that MPK4 is found in complexes *in vivo* with PAT1, a component of the mRNA decapping machinery. PAT1 is also phosphorylated by MPK4 and, upon flagellin PAMP treatment, PAT1 accumulates and localizes to cytoplasmic processing (P) bodies which are sites for mRNA decay. *Pat1* mutants exhibit dwarfism and de-repressed immunity dependent on the immune receptor SUMM2. Since mRNA decapping is a critical step in mRNA turnover, linking MPK4 to mRNA decay via PAT1 provides another mechanism by which MPK4 may rapidly instigate immune responses.

Keywords decapping; immunity; MAP kinases; mRNA decay; phosphorylation
Subject Categories Microbiology, Virology & Host Pathogen Interaction; Plant Biology; RNA Biology
DOI 10.15252/embj.201488645 | Received 2 April 2014 | Revised 2 December 2014 | Accepted 11 December 2014 | Published online 20 January 2015
The EMBO Journal (2015) 34: 593–608

Introduction

Plant innate immunity employs multilayered defense responses comprised of two overlapping mechanisms. In the first layer, plant pattern recognition receptors detect invading microorganisms by the presence of conserved pathogen-associated molecular patterns (PAMPs) (Boller & Felix, 2009). PAMP recognition is exemplified by the binding of the bacterial flagellin-derived flg22 peptide to the leucine-rich repeat-receptor-like kinase flagellin sensing 2 (FLS2) (Gomez-Gomez *et al*, 2001; Chinchilla *et al*, 2006). PAMP recognition initiates downstream signaling, including production of reactive oxygen species, calcium influx, MAP kinase activation and global changes in gene expression that induce PAMP-triggered immunity (PTI) (Chisholm *et al*, 2006; Zipfel, 2009). Adapted pathogens have evolved effector proteins that are delivered into host cells to compromise PTI by evading PAMP detection or suppressing defense responses. In the second layer of immunity, plant resistance (R) proteins have evolved to directly or indirectly recognize the activities of pathogen effectors (Jones & Dangl, 2006). In the best-studied examples, R proteins are found to guard host proteins or complexes (guardees) manipulated by specific pathogen effectors. Pathogen detection via R proteins leads to induction of strong defenses and to a form of host programmed cell death known as the hypersensitive response (HR) to sequester infections. These responses are collectively termed effector-triggered immunity (ETI) (Jones & Dangl, 2006).

Changes in phosphorylation are important regulatory mechanisms in cellular signaling. Activation of mitogen-activated protein (MAP) kinases occurs within 10 min of PAMP application (Asai *et al*, 2002; Boller & Felix, 2009) and relies on sequential phosphorylations between MAPKK-kinases (MEKK), MAPK kinases (MKK) and MAP kinases (MPK) (Pitzschke *et al*, 2009; Andreasson & Ellis, 2010; Rasmussen *et al*, 2012). In *Arabidopsis*, several MPKs are activated by PAMPs. A cascade comprising MEKK1-MKK4/5-MPK3/6 was initially found to be involved in PTI downstream of FLS2 (Asai *et al*, 2002; Droillard *et al*, 2004; Gao *et al*, 2008). Similarly, flg22 treatment activates another cascade including MEKK1, MKK1/2 and MPK4 (Petersen *et al*, 2000; Ichimura *et al*, 2006; Mészáros *et al*, 2006; Suarez-Rodriguez *et al*, 2007; Gao *et al*, 2008; Qiu *et al*, 2008a).

1 Department of Biology, Faculty of Science, University of Copenhagen, Copenhagen, Denmark
2 New England Biolabs Ltd, Whitby, ON, Canada
3 Department of Plant Biology, University of Minnesota, St. Paul, MN, USA
4 Department of Biology, University of Utah, Salt Lake City, UT, USA
5 University of Southern Denmark, Institute for Biochemistry and Molecular Biology, Odense, Denmark
*Corresponding author. Tel: +45 353 22127; E-mail: shutko@bio.ku.dk
†These authors contributed equally to this work

© 2015 The Authors

Interestingly, Flg22-induced activation of MPK3, MPK4 and MPK6 is dependent on MKK1, while MPK3 and MPK6 are also activated by MKK4 (Mészáros *et al*, 2006). Thus, FLS2 activates two cascades, one with an unknown MEKK and MKK4/5-MPK3/6, the other with MEKK1-MKK1/2-MPK4. More recently, the closest homologue of MPK4, MPK11, was shown to also be activated by PAMPs (Bethke *et al*, 2012).

mpk4 mutants were originally found to exhibit autoimmunity, and MPK4 thus appeared to function genetically as a negative regulator of defense responses (Petersen *et al*, 2000; Droillard *et al*, 2004). However, MPK4 is activated in response to pathogens and PAMP elicitation (Droillard *et al*, 2004; Teige *et al*, 2004; Ichimura *et al*, 2006; Brader *et al*, 2007; Qiu *et al*, 2008a) which is counter-intuitive for a negative regulator. Subsequently, it was shown that activated MPK4 interacts with and phosphorylates MAP kinase substrate 1 (MKS1), bringing about the release of the transcription factor WRKY33 and induction of the expression of the *PHYTOALEXIN DEFICIENT 3* (*PAD3*) gene required for biosynthesis of the antimicrobial camalexin (Andreasson *et al*, 2005; Qiu *et al*, 2008b). This illustrates how MPK4 functions as a positive regulator of PTI. Since it was recently reported that MPK4 is a target for manipulation by pathogen effectors (Zhang *et al*, 2007, 2012), and as *mpk4* mutant phenotypes are partially suppressed by mutations in the R protein SUMM2 (suppressor or *mkk1 mkk2*) (Zhang *et al*, 2012), one model is that MPK4 is a PTI guardee whose absence triggers ETI.

Apart from regulation by transcription factors, mRNA translation and degradation also regulate gene expression, especially when they are reprogrammed to stabilize bulk mRNAs and favor mRNAs required for an appropriate stress response (Jiao *et al*, 2010; Munchel *et al*, 2011; Park *et al*, 2012; Ravet *et al*, 2012). mRNA is intrinsically unstable to facilitate rapid changes in mRNA abundance in response to stimuli. Eukaryotic mRNAs contain stability determinants including the 5′ 7-methylguanosine triphosphate cap (m7G) and the 3′ poly(A) tail. To achieve fine control of transcript abundance, mRNA is attacked by a decapping complex that breaks down RNA in a coordinated manner. mRNA decay is initiated by deadenylation, the removal of the 3′ poly(A) tail, whereafter mRNA can either be routed to 3′–5′ degradation by exosomal exonucleases, or 5′–3′ by the exoribonuclease activity of the decapping complex (Garneau *et al*, 2007). The decapping complex is highly conserved among eukaryotes (Garneau *et al*, 2007; Xu & Chua, 2011) and comprises the decapping enzyme DCP1/2 which removes the 5′ m7G cap, and the exoribonuclease XRN that degrades the monophosphorylated mRNA. Deadenylation and decapping are linked in eukaryotes by the decapping enhancer PAT1 (protein associated with topoisomerase II) (Hatfield *et al*, 1996; Wang *et al*, 1996; Tharun & Parker, 2001; Ozgur *et al*, 2010). In yeast, PAT1 promotes the interaction between mRNA and decapping enzyme, altering the messenger ribonucleoprotein (mRNP) organization from an arrangement favoring translation to one promoting decay. mRNA decay occurs in distinct cytoplasmic foci called processing bodies (PBs) in eukaryotes (Parker & Sheth, 2007; Balagopal & Parker, 2009), where mRNPs are sequestered for degradation, or from which they may re-enter polysomal complexes (Brengues, 2005). PBs can also harbor translationally arrested mRNPs and RNA silencing machinery (Balagopal & Parker, 2009; Xu & Chua, 2009; Thomas *et al*, 2011).

In plants, the decapping machinery includes the decapping enzyme DCP2 and its activators DCP1, DCP5, VARICOSE (VCS) (Deyholos *et al*, 2003; Xu *et al*, 2006; Goeres *et al*, 2007; Brodersen *et al*, 2008; Xu & Chua, 2009, 2011; Motomura *et al*, 2012) as well as the exoribonuclease XRN4 (Olmedo *et al*, 2006; Potuschak *et al*, 2006; Gregory *et al*, 2008; Rymarquis *et al*, 2011; Vogel *et al*, 2011). It is thought that DCP1, DHH1 and DCP5 form mRNPs for translational repression of target mRNA, which are then subject to decapping by recruitment of DCP2 and VCS and digestion by XRN4 (Xu & Chua, 2009, 2011). Importantly, although PAT1 functions have not previously been studied in plants, three homologues are encoded in the *Arabidopsis* genome, each of which contains a conserved C-terminal domain. The decapping activator Sm-like (LSM) proteins, which interact with PAT1 in eukaryotes (Salgado-Garrido *et al*, 1999; Bonnerot *et al*, 2000; Bouveret *et al*, 2000; Tharun *et al*, 2000; Tharun, 2009), have recently been characterized in *Arabidopsis* (Perea-Resa *et al*, 2012; Golisz *et al*, 2013). It was found that LSM1-7 proteins form a complex and *lsm1* mutants accumulate capped mRNA. Furthermore, VCS, DHH1 and PAT1 homologs were identified in LSM1 immunoprecipitates (Golisz *et al*, 2013).

The decapping complex plays important roles in eukaryotic development. In contrast, links between mRNA decapping and stress signaling are just being uncovered (Jiao *et al*, 2010; Buchan *et al*, 2011; Munchel *et al*, 2011; Park *et al*, 2012), and how decapping may be involved in regulating immune systems is largely unknown. Here, we characterize the *Arabidopsis* homologue of the mRNA decay regulator PAT1. We show that PAT1 functions in decapping of mRNA. Furthermore, PAT1 is phosphorylated in response to flg22 and localizes to discrete, punctate foci in the cytosol. PAT1 also interacts with MPK4 and with the R protein SUMM2 *in planta*, and the absence of PAT1 triggers SUMM2 dependent immunity. This indicates that PAT1 is regulated by MPK4 in a pathway whose disruption leads to ETI via SUMM2.

Results

AtPAT1 is an ScPAT1 orthologue and interacts with MPK4 *in planta*

We previously conducted a yeast two-hybrid screen to identify *Arabidopsis* proteins that interact with MPK4 (Andreasson *et al*, 2005). In addition to the MPK4 substrate MKS1, we identified two clones encoding PAT1 (At1g79090), an mRNA decapping stimulator involved in post-transcriptional gene regulation (Coller & Parker, 2005). Two PAT1 homologs are encoded in the *Arabidopsis* genome (*AtPAT1H1* At3g22270; *AtPAT1H2* At4g14990, Supplementary Fig S1A). The steady-state expression level of PAT1 and the homologs compared to the housekeeping gene *ACTIN8* (At1g49240) was analyzed by RT-PCR (Supplementary Fig S1B). We focused on PAT1 as the other two homologs were not identified by yeast two-hybrids. To confirm the PAT1-MPK4 interaction *in planta*, doubly transgenic *Arabidopsis* lines were generated in the L*er mpk4-1* background that expressed PAT1 with a C-terminal Myc tag and HA-tagged MPK4 under the control of their own promoters. Anti-Myc immunoprecipitation from either MPK4-HA or double transgenic MPK4-HA/Pat1-Myc tissue detected a 50 kDa band corresponding to MPK4-HA only in double transgenic lines (Fig 1A). Thus, MPK4 and PAT1 can be found in complex in *Arabidopsis*.

 © 2015 The Authors

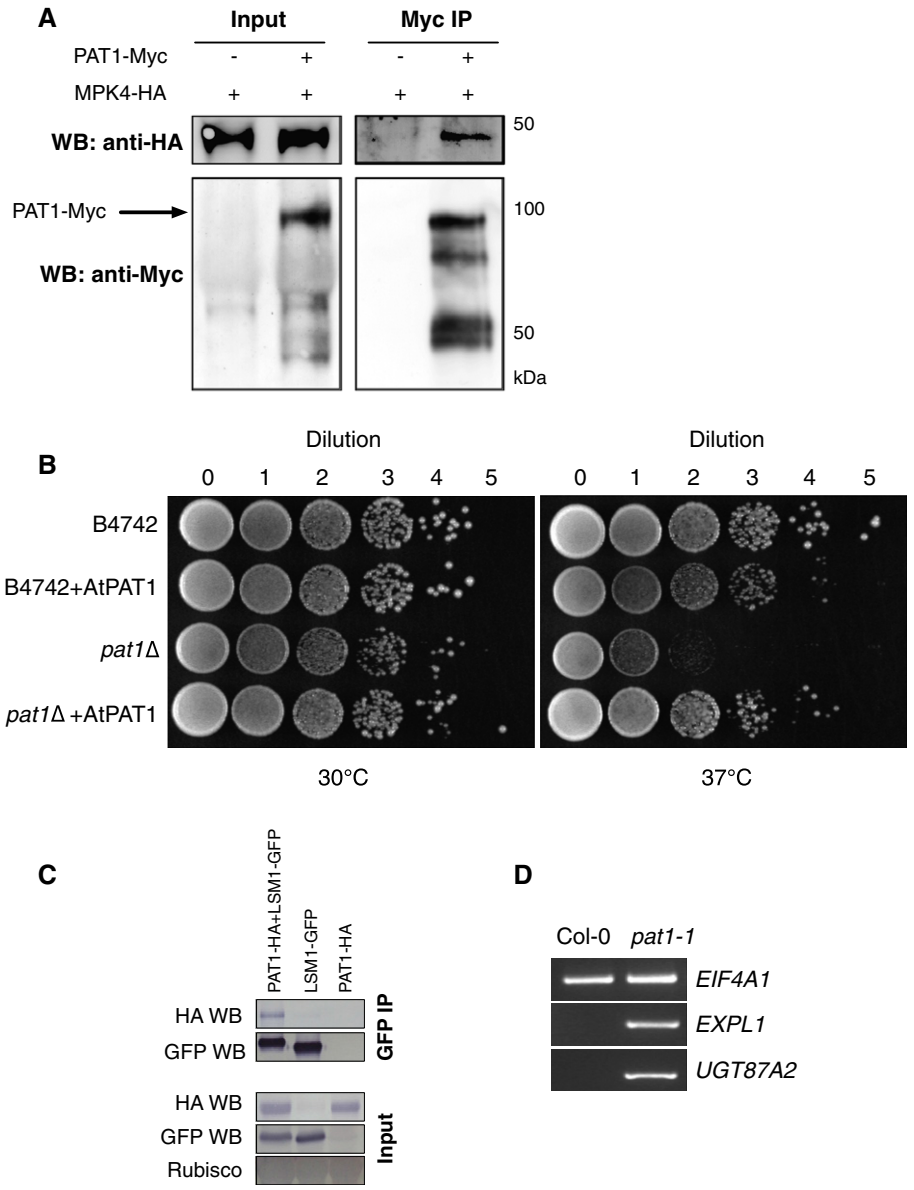

Figure 1. MPK4 and PAT1 interact in *Arabidopsis*.

A MPK4-HA is detected in PAT1-Myc immunoprecipitates from double transgenic *Arabidopsis* plants. Immunoblots of input and anti-Myc IPs probed with anti-HA and anti-Myc antibodies. Left panel, input; right panel, anti-Myc IP.

B Yeast *pat1*Δ mutants are unable to grow at 37°C while wild-type (B4742) strain grows at 30°C (left panel) and 37°C (right). Growth at 37°C is restored in *pat1*Δ expressing *AtPAT1*. Serial dilutions of each yeast strain were plated on YPAD agar plates and grown at the indicated temperatures.

C Co-IP between PAT1-HA and LSM1-GFP. Proteins were transiently co-expressed in *N. benthamiana* and tissue harvested 3 days post-infiltration. Immunoblots of GFP IPs (top panel) and inputs (20 μg each, bottom panel). Immunoblots were cut in half and probed with anti-HA antibodies and anti-GFP antibodies.

D Agarose gel electrophoresis of 5′ RACE PCR to detect capped transcripts of *EIF4A1*, *UGT87A2* and *EXPL1* in 14-day-old Col-0 and *pat1-1*.

Source data are available online for this figure.

Yeast PAT1 engages with translating mRNPs and is involved in translational repression and decapping activation (Marnef & Standart, 2010). Since the function of PAT1 in *Arabidopsis* was unknown, we examined whether it functions similarly to yeast PAT1. To this end, a full-length *Arabidopsis PAT1* cDNA was cloned from Col-0 (Supplementary Fig S1C and D) and transformed into wild-type yeast (B4742) and a yeast mutant (Y15797) in which yeast *PAT1* was replaced with a G418 resistance cassette (BY4742 (YCR077c) *pat1*Δ::*KanMX*). In contrast to the wild-type, yeast lacking PAT1 (*pat1*Δ) display a temperature-sensitive phenotype and are impaired at 37°C but grow normally at 30°C (Tharun *et al*, 2005). This phenotype is reverted to wild-type in yeast containing *Arabidopsis PAT1*, as growth at 37°C was restored (Fig 1B). As an additional control, we transformed *Arabidopsis PAT1* into wild-type

© 2015 The Authors

yeast (B4742/AtPAT1), and this grew similarly to wild-type at 30°C and almost as well at the wild-type at 37°C (Fig 1B). The expression of *Arabidopsis* PAT1 in yeast was confirmed by anti-PAT1 immunoblotting of yeast protein extracts (Supplementary Fig S1E). This provides compelling evidence for the orthologous functions of these yeast and *Arabidopsis* PAT1 proteins. As PAT1 is found in complex with MPK4, these results provide a link between MPK4 and post-transcriptional regulation of mRNA stability.

We next analyzed the interaction between PAT1 and conserved components of mRNA decapping. PAT1-LSM1-7 complexes function in mRNA decapping and deadenylation (Bouveret *et al*, 2000; Tharun, 2009; Haas *et al*, 2010; Ozgur *et al*, 2010; Totaro *et al*, 2011). We therefore transiently expressed in *Nicotiana benthamiana* LSM1-GFP and PAT1-HA and then immunoprecipitated LSM1 with GFP Trap beads. PAT1-HA could be detected in LSM1 immunoprecipitates but did not adhere to GFP Trap beads in the absence of LSM1-GFP (Fig 1C). This is consistent with the detection of peptides corresponding to PAT1 and its homologues in LSM1 immunoprecipitates (Golisz *et al*, 2013) and supports a role of PAT1 in mRNA decapping. In other organisms, interactions between PAT1 and LSM1 are robust, while those between PAT1 and other mRNA decapping proteins, including the DCP1-DCP2 complex and XRN1, are more transient (Bouveret *et al*, 2000; Nissan *et al*, 2010; Ozgur *et al*, 2010). This is consistent with our difficulty in detecting DCP1 in complex with PAT1 in *Arabidopsis* (Supplementary Fig S1F).

PAT1 is required for decapping of selected mRNAs

In order to determine whether PAT1 behaves as an activator of mRNA decapping, we used 5′ RACE to compare the levels of capped mRNAs in Col-0 and *pat1* mutants. To this end, we identified an allele, *pat1-1* (Salk_040660), with a T-DNA insertion in the last exon of *PAT1* (Supplementary Fig S1C). We also generated an anti-PAT1 antibody against a C-terminal peptide (Supplementary Fig S1D). Immunoblotting of Col-0 protein extracts with this antibody detected a clear band around 90 kDa. In contrast, no protein could be detected in *pat1-1* mutant extracts (Supplementary Fig S1G). This indicates that *pat1-1* harbors either a truncated version of PAT1, no PAT1 protein, or levels of the protein that are below detection.

5′ RACE was performed on transcripts known to be degraded by the decapping complex (*EXPL1*; *UGT87A2*) (Perea-Resa *et al*, 2012), as well as a housekeeping transcript *EIF4A1*. We found that capped *EXPL1* and *UGT87A2* accumulated in *pat1-1* mutants, while capped *EIF4A1* mRNA was present in equal amounts in Col-0 and *pat1-1* (Fig 1D). This indicates that PAT1 plays a role in mRNA decay via decapping.

PAT1 is an MPK4 substrate

Since MPK4 and PAT1 are found in complexes *in planta*, we asked whether PAT1 is an MPK substrate. PAT1 contains 5 Ser-Pro (SP) motifs which are commonly phosphorylated by MPKs (Pearson *et al*, 2001; Ubersax & Ferrell, 2007) (Supplementary Fig S1D). To characterize PAT1 phosphorylation *in vivo*, we identified PAT1 phosphopeptides by mass spectrometry. Since MPK3/4/6 are activated by flagellin and by virulent strains of *Pseudomonas syringae* pv. *tomato* (*Pto*) DC3000 (Asai *et al*, 2002; Brader *et al*, 2007; Suarez-Rodriguez *et al*, 2007; Bethke *et al*, 2009, 2012; Rasmussen *et al*, 2012), PAT1 was immunoprecipitated from extracts of untreated control and flg22-treated wild-type Col-0 or PAT1-GFP transgenic lines. Bands corresponding to PAT1-GFP (130 kDa) were excised from the gel (Supplementary Fig S2), subjected to in-gel tryptic digestion, and peptides were extracted. Phosphopeptides were enriched by TiO_2 chromatography and analyzed by liquid chromatography (RP-HPLC) coupled to electrospray ionization tandem mass spectrometry (LC-ESI-MS/MS). This identified several phosphopeptides from PAT1-GFP IPs that were not detectable in the negative control (Col-0) (Table 1; Supplementary Fig S2). The most abundant phosphopeptide, based on the extracted ion chromatogram from the LC-MS/MS analysis, revealed phosphorylation of Ser208 in an SP motif (Fig 2A). Another peptide was identified with phosphorylation of Ser343. However, this site is not within an SP motif, making it a less likely site for phosphorylation by MPKs. Importantly, both these peptides have previously been detected in *Arabidopsis* by mass spectrometry (Phosphat Database, http://phosphat.mpimp-golm.mpg.de/). It should be noted that the PAT1 phosphopeptides were detected both whether or not the sample had been treated with flg22. Thus, under the conditions used here, PAT1 was phosphorylated and remained so after exposure to flg22.

To determine whether PAT1 is a substrate of a specific MPK, we carried out *in vitro* kinase assays using immunoprecipitated, PAMP-activated MPKs with purified His_6-PAT1 protein. Phosphorylated His_6-PAT1 was detectable as a radioactive band around 95 kDa after incubation with flg22-activated MPK4 (Fig 2B), while MPK6 caused only low levels of PAT1 phosphorylation and MPK3 did not significantly alter PAT1 phosphorylation (Supplementary Fig S3). Each MPK was also incubated with the generic MPK substrate myelin basic protein (MBP) to verify their activation (Fig 2B; Supplementary Fig S3). This confirms that activated MPK4, and to a lesser extent, MPK6, is responsible for the phosphorylation of PAT1. A version of His_6-PAT1 with Ser208 mutated to alanine (S208A) was also incubated with MPK4 and MPK6 IPs, and this mutant

Table 1. Phosphopeptides identified in PAT1-GFP IPs by mass spectrometry analysis.

Sequence	Phospho-sites[a]	m/z	Mascot score	
			PAT1GFP water	PAT1GFP flg22
SSFVSYPPPGSI**S**PDQR	1 (S208)	950.93005	71	79
SSFV**S**YPPPGSI**S**PDQR	2 (S208, S200)	990.91333	46	64
SS**S**GNYDGMLGFGDLR	1 (S343)	929.87323	70	114
S**SS**GNYDGMLGFGDLR	2 (S343, S342)	969.85663	39	50

[a]Phosphosites refers to the number and in brackets the location of the phosphorylation detected by MS analysis. Potential phosphorylation sites are indicated in bold letters. m/z refers to the mass-to-charge ratio of the tabulated peptides.

 © 2015 The Authors

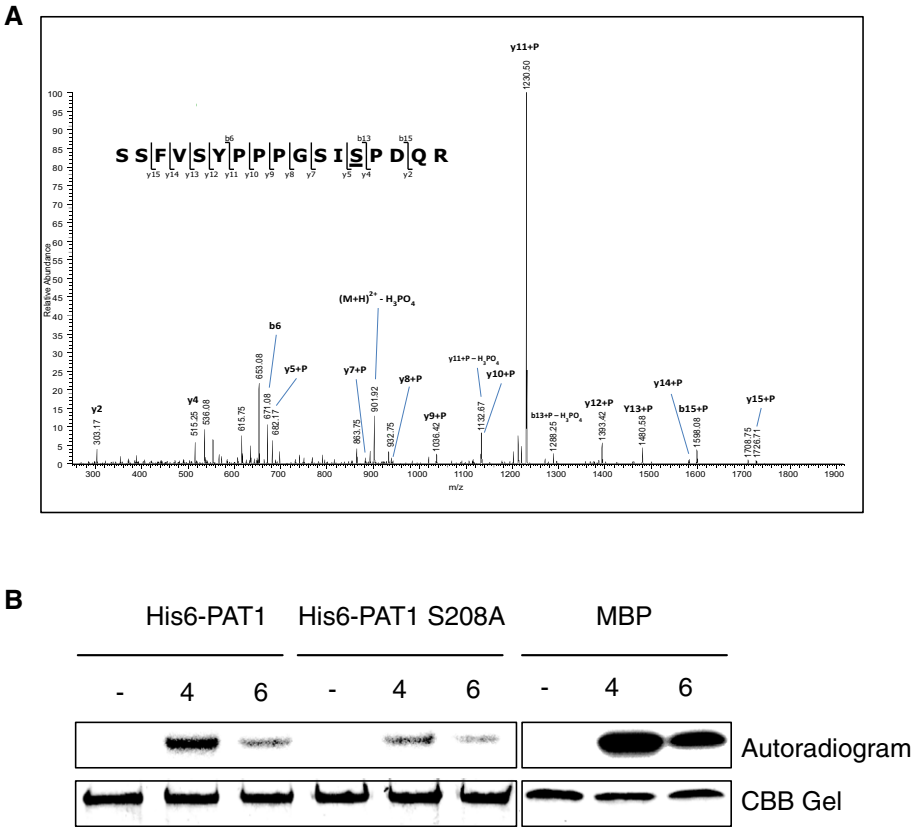

Figure 2. PAT1 is phosphorylated *in planta* and *in vitro*.

A Tandem MS spectrum of the phosphopeptide SSFVSYPPPGSISPDQR in which the underlined serine is phosphorylated. Y- and b-ions are indicated that localize phosphorylation to the SP site.

B MPK4 and MPK6 were immunoprecipitated from extracts of Col-0 seedlings treated with 200 nM flg22 for 10 min. For the negative control (–), extracts were incubated with agarose beads without antibodies. IPs were incubated with His_6-PAT1, His_6-PAT1 S208A or MBP for 60 min at 37°C before boiling and SDS-PAGE. Autoradiogram (top panel), Coomassie-stained gel for loading control (bottom).

Source data are available online for this figure.

had significantly lower levels of phosphorylation (Fig 2B). This supports the identification of S208 as a key phosphorylation site in PAT1.

pat1 mutants exhibit autoimmunity similar to *mpk4*

Given that MPK4 is an important immune regulator in *Arabidopsis* and that *mpk4* mutants have de-repressed defense responses, we examined whether PAT1 may also be involved in immunity. The *pat1-1* mutant has a distinct leaf serration phenotype and a slightly smaller rosette than Col-0 (Fig 3). A similar rosette phenotype was seen in another T-DNA insertion line (*pat1-2*, WiscDsLox_734_D04 in Supplementary Figs S1C and S4), indicating that this phenotype is due to loss-of-function of PAT1. Importantly, however, the phenotype of *pat1-1* is not as extreme as *mpk4-2*, which is much smaller and has more pronounced leaf curling and reduced fertility as well as constitutive defense gene expression (Petersen *et al*, 2000); Fig 3).

In order to determine whether *pat1-1* is a constitutive defense mutant similar to *mpk4*, quantitative reverse-transcription PCR (qRT-PCR) was used to measure the steady-state level of the pathogenesis-related *PR1* and *PR2* genes in adult plants (Fig 4A). Previous work showed that the enhanced defense response of *mpk4* mutants is suppressed by mutations in EDS1 (Brodersen *et al*, 2006). Thus, *eds1-2* was crossed with *pat1-1* to explore the *pat1* phenotype in the absence of this regulator (Fig 3). Compared to Col-0, *pat1-1* mutants accumulated 1,000-fold more *PR1* and 150-fold more *PR2* transcripts (Fig 4A). In contrast, the levels of *PR* mRNAs in *pat1-1 eds1-2* double mutants were similar to those in wild-type (Fig 4A). Under the same conditions, *mpk4-2* mutants accumulated 4,000-fold more *PR1* and 800-fold more *PR2* transcripts (Fig 4A).

We found that the elevated *PR* gene expression in *pat1-1* correlated to an enhanced resistance to infection by syringe-infiltrated *Pto* DC3000 when compared to Col-0 (Fig 4B). While *Pto* DC3000 growth reached 5.5 cfu/cm^2 in Col-0, *pat1-1* mutants supported tenfold lower accumulation of *Pto* DC3000. In this experiment, *eds1-2* mutants showed enhanced bacterial growth as expected for this mutant with compromised defense responses (Fig 4B). *pat1* disease resistance is EDS1 dependent, as bacterial growth *pat1-1 eds1-2* double mutants was similar to that in *eds1-2* (Fig 4B). These findings indicate that, similar to *mpk4*, *pat1* mutants express EDS1-dependent autoimmunity in the absence of microbes.

© 2015 The Authors

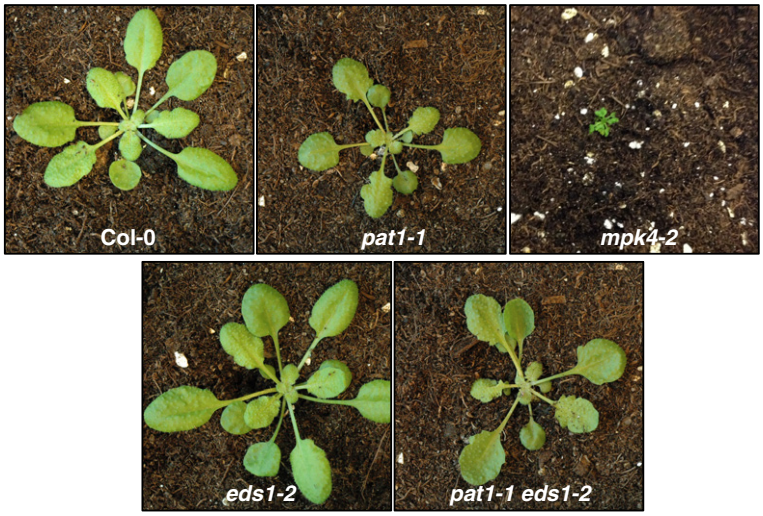

Figure 3. *pat1* mutants have a serrated leaf, semi-dwarf phenotype.
Plants photographed at 4 weeks of growth in short day conditions, genotypes as indicated. Col-0 and *eds1-2* plants and *pat1-1* and *pat1-1/eds1-2*, respectively, were placed in the middle of the same pots before the pictures were taken.

PAT1 detection in P-bodies is induced by PAMPs

Processing bodies (PBs) are cytoplasmic granules involved in both mRNA decay and translational repression pathways (Kulkarni *et al*, 2010). PAT1 is a conserved PB component in yeast (Rodriguez-Cousino *et al*, 1995), *C. elegans* (Boag *et al*, 2008), *Drosophila* (Marnef *et al*, 2010) and mammals (Scheller *et al*, 2007) and PBs can be significantly induced in *Arabidopsis* by hypoxia and heat stress (Weber *et al*, 2008). To investigate whether PAT1 is found in PBs, we produced transgenic *Arabidopsis* lines that express PAT1-GFP from its native promoter complementing the *pat1* phenotype (Supplementary Fig S5A and B). We detected GFP signal in small numbers of distinct foci by confocal microscopy in roots of young seedlings (Fig 5A). Within 20 min of flg22 treatment, a significant increase in the number of GFP-positive foci could be seen in the root tips (Fig 5A). To test whether these foci correspond to PBs, we treated the roots with cycloheximide in DMSO which is known to abrogate PB formation in plants (Goeres *et al*, 2007). This revealed that cycloheximide inhibited flg22-induced foci (Fig 5A). Importantly, the control DMSO treatment did not reduce the number of foci (Supplementary Fig S6A and B). As a control, we also tracked the localization of the known decapping component VCS (Xu *et al*, 2006). Similar to PAT1-GFP, VCS-GFP was seen in flg22-induced PBs and absent when treated with cycloheximide (Fig 5B). Interestingly, PAT1 protein, which is hardly detectable under steady-state conditions, also accumulated in response to flg22 treatment, with a peak by 60 min, and a return to normal levels after 2 h (Fig 5C). PAT1-GFP mirrors this effect and was similarly up-regulated in response to flg22 treatment, as detected by anti-GFP Western blotting of seedling protein (Fig 5D). Importantly, *PAT1* transcript levels were not highly induced by flg22 treatment in Col-0 seedlings (Supplementary Fig S6C), suggesting that PAT1 induction occurs post-transcriptionally. These data indicate that activation of PTI leads to up-regulation of PAT1 protein levels by an unknown post-transcriptional mechanism, and this facilitates the detection of PAT1 in PBs. In addition, PTI could induce PB formation as part of cellular reprogramming, and PAT1 may localize to PBs to engage in this process.

The MPK4 suppressor *summ2* also suppresses the *pat1* resistance phenotype

Autoimmunity caused by loss of different components of the MPK4 kinase cascade can be suppressed by mutations in the resistance protein SUMM2 (Zhang *et al*, 2012). An explanation for this is that SUMM2 keeps this PAMP responsive pathway under surveillance and that mutations in its components mimic the effects of microbial effectors that prevent phosphorylation within or below the cascade (Zhang *et al*, 2007). To further probe the connection between MPK4 and PAT1, we generated *pat1-1 summ2-8* double mutants. These mutants retained the leaf serration phenotype of *pat1-1* single mutants (Supplementary Fig S7A). However, double mutants no longer accumulated excessive *PR1* and *PR2* transcripts (Fig 6A) and displayed *summ2* levels of susceptibility to syringe-infiltrated *Pto* DC3000 (Fig 6B). Importantly, the *pat1* growth phenotype was not caused by overexpression of *SUMM2* transcripts, as the level of *SUMM2* in *pat1-1* was similar to wild-type (Supplementary Fig S7B). To test whether the accumulation of 5′ capped transcripts in *pat1-1* (Fig 1D) was merely an effect of inappropriate activation of SUMM2, we tested the accumulation of 5′ capped *UGT87A2* in an XRN1 sensitivity assay. XRN1 degrades all uncapped RNA leaving 5′ capped RNA intact (Blewett & Goldstrohm, 2012). The accumulation of 5′ capped versus uncapped *UGT87A2* transcripts was at similar levels in *pat1-1* and *pat1-1 summ2-8* (Fig 6C). Col-0 and *summ2-8* plants had similarly reduced 5′ capped versus uncapped ratios but, importantly, these were much lower than the levels of *pat1-1* and *pat1-1 summ2-8* (Fig 6C). Therefore, the accumulation of capped transcripts in *pat1-1* mutants is not an artifact of defense activation but reflects a role for PAT1 in mRNA decay. In order to determine whether the SUMM2-mediated resistance in *pat1* mutants is specific to pathogens of a specific class, we compared susceptibility to pathogens with different lifestyles. *Pto* DC300 is a hemi-biotrophic

 © 2015 The Authors

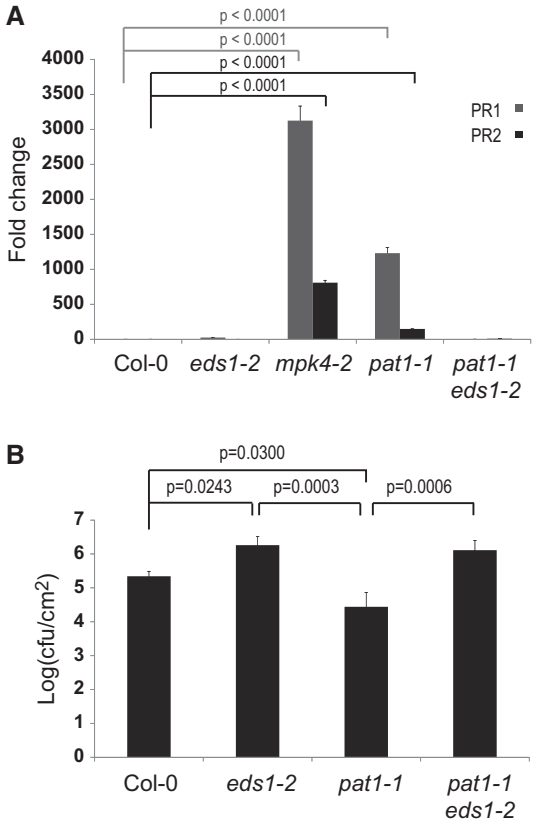

Figure 4. *pat1* mutants display EDS1-dependent, constitutive defense responses.

A *PR* gene expression is elevated in *mpk4-2* and *pat1-1* mutants. Four-week-old plants were used for RNA extraction, followed by qRT-PCR. Fold-change in *PR1* (gray bars) and *PR2* (black) expression is relative to Col-0, normalized to *UBQ10*. Standard error of the mean is indicated by errors bars (n = 3). Statistical significance between the mean values was determined by ANOVA followed by Fisher's LSD test, P-values are only shown for mean values significantly different from Col-0.

B *pat1* is more resistant to colonization by *P. syringae* pv. *tomato* DC3000. Bacteria were syringe-infiltrated and samples taken 3 days post-infiltration. Data are shown as $\log_{10}$-transformed colony-forming units/cm^2 leaf tissue (cfu/cm^2). Standard error of the mean is indicated by errors bars (n = 4). Statistical significance between the mean values was determined by ANOVA followed by Fisher's LSD test.

pathogen, which grows in living tissue during early infection. In contrast, the necrotrophic fungal pathogen *Botrytis cinerea* relies on dying tissue for its propagation in plants (Glazebrook, 2005). Infection of *pat1-1 summ2* double mutants with *B. cinerea* resulted in similar growth of the fungus as detected in *summ2-8* single mutants (Supplementary Fig S8).

To more accurately address to what extent PAT1 phosphorylation is MPK4 dependent and to measure PAT1 phosphorylation profiles before and after flg22 treatment, we generated PAT1-HA transgenic lines in the *mkk1/2 summ2-8* background. The suppression of *mpk4* by *summ2-8* is only partial, but the autoimmunity phenotype is fully suppressed in *mkk1/2 summ2* triple mutants. We next applied quantitative mass spectrometry (iTRAQ) to PAT1-HA IPs from Col-0 and *mkk1/2-summ2* and this revealed increased phosphorylation stoichiometry of PAT1 at Ser208 in untreated Col-0 compared to *mkk1/2 summ2* plants (Fig 6D). Flg22 treatment leads to increased levels of PAT1 Ser208 in both genotypes, but the levels in Col-0 were higher than what we found for PAT1 in *mkk1/2 summ2* (Fig 6D). Since flg22 treatment augments PAT1 Ser208 phosphorylation in the absence of MKK1/2, MPK4 might be activated by other upstream kinases or PAT1 may be phosphorylated by MPK6. Nevertheless, these data indicate that flg22 treatment leads to increased phosphorylation of PAT1 at Ser208 and the MKK1/2 MPK4 pathway contributes to this phosphorylation.

Our data indicate that PAT1 is part of the pathway including MPK4 and the SUMM2 R protein. SUMM2 and PAT1 might thus interact *in planta*. To test this, we transiently expressed and immunoprecipitated PAT1-GFP in *N. benthamiana* also transiently expressing MPK4-HA or SUMM2-HA. When PAT1-GFP was pulled down using GFP Trap beads, we could easily detect MPK4-HA and SUMM2-HA in the immunoprecipitates (Fig 7A). To verify the association of MPK4, SUMM2 and LSM1, we also pulled down PAT1-HA and detected MPK4-GFP, SUMM2-GFP and LSM1-GFP in the immunoprecipitates but not Myc-GFP (Supplementary Fig S9). To further confirm the association of PAT1 and SUMM2, we used bimolecular fluorescence complementation (BiFC), which produces a fluorescent readout upon reconstruction of YFP. The BiFC assay showed detectable YFP signal in the cytoplasm when PAT1 and SUMM2 were co-expressed (Fig 7B). No signals were observed when PAT1 was expressed with another R protein, At4g12010, implying that the association/reconstruction is specific (Fig 7B, bottom panel). This indicates that PAT1 is in complex with SUMM2 *in planta*. Thus, MPK4 and PAT1 are both physically and genetically linked to SUMM2.

Discussion

In this study, we identify the *Arabidopsis* decapping component PAT1 and show it to be an interactor and substrate of MPK4 in plant innate immunity. Furthermore, we demonstrate that *Arabidopsis* PAT1 complements yeast *pat1*Δ mutants, indicating that the function of this conserved protein is maintained in plants. The accumulation of capped mRNAs in *pat1* mutants is consistent with a role for PAT1 in the mRNA decapping pathway.

Pat1 mutants exhibit a distinct leaf serration phenotype (Supplementary Fig S4) resembling those of miRNA-loss-of-function mutants (Nikovics *et al*, 2006) such as *abh1-8* (Gregory *et al*, 2008), *serrate* (Grigg *et al*, 2005) and hypomorphic alleles of *ago1* (Morel, 2002). This suggests that PAT1 may have a role connected to microRNA activity. *Arabidopsis* decapping mutants such as *dcp1*, *dcp2* and *vcs* accumulate lower levels of certain miRNAs (Motomura *et al*, 2012). Mutants with a *pat1*-like phenotype, such as *vcs, suo6* and *amp1*, have revealed new components in miRNA-mediated translational repression (Brodersen *et al*, 2008; Yang *et al*, 2012; Li *et al*, 2013). In *Drosophila*, HPat interacts with components of the miRNA machinery including AGO1 and GW182 (Barišić-Jäger *et al*, 2013). The connection between the mRNA decay activator HPat and the miRNA effector complex may provide a link to promote the transition of mRNA from translation to degradation. Although PAT1 may regulate targets of miRNA-mediated translational repression, the mechanism by which translational repression occurs in *Arabidopsis* is still under investigation.

© 2015 The Authors

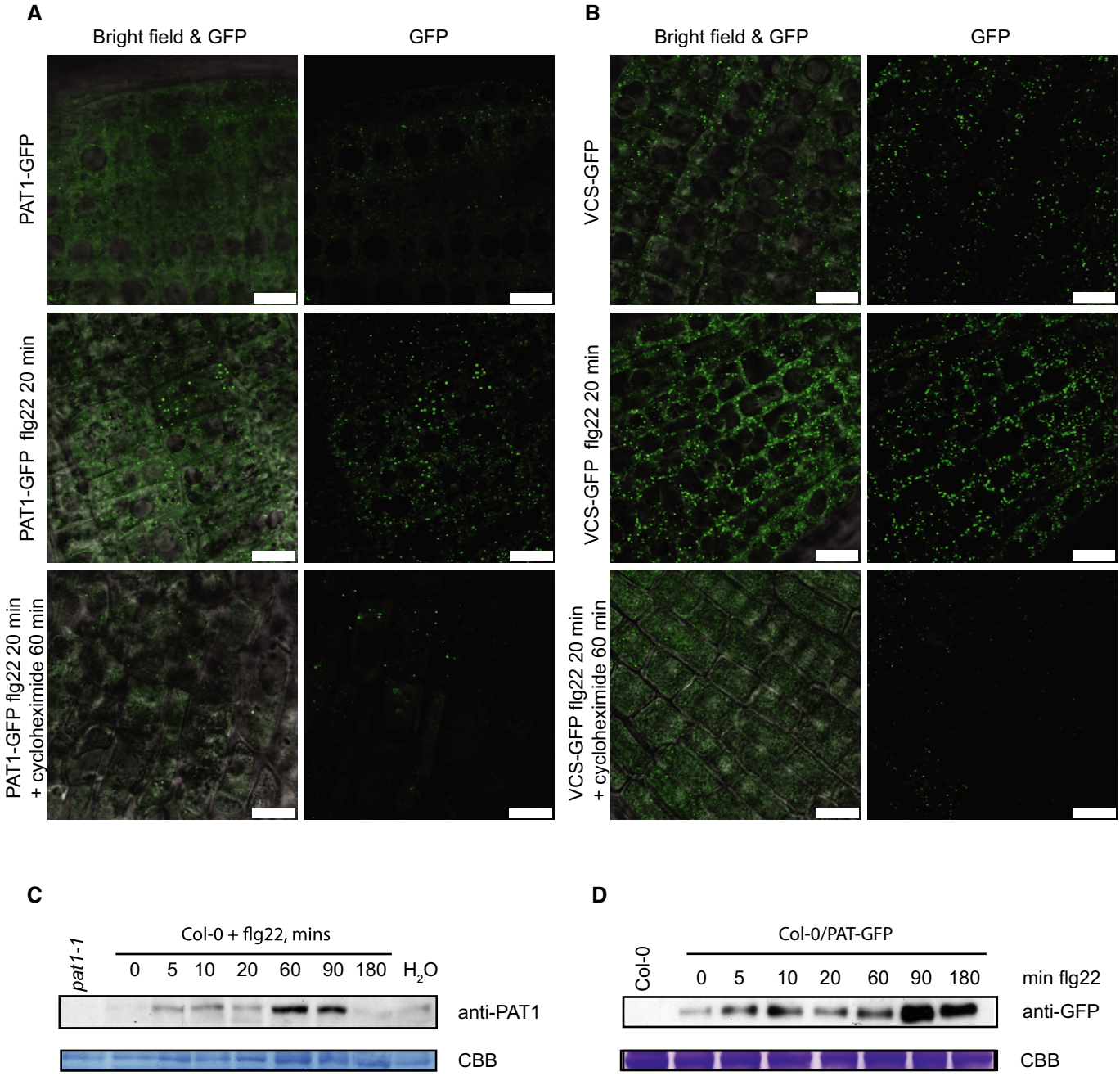

Figure 5. PAT1-GFP is present in P-bodies after PAMP treatment.

A Confocal microscopy with root elongation zones. Five-day-old Col-0/PAT1-GFP seedlings were treated with 1 μM flg22 on glass slides for 20 min (second panel) followed by treatment with 100 μg/ml cycloheximide for 60 min (bottom panel). The scale bar corresponds to 10 μm.

B Confocal microscopy with 5-day-old VCS-GFP seedlings treated as in (A). The scale bar corresponds to 10 μm.

C PAT1 protein is induced by PAMP treatment. Immunoblot detection of equal amounts of protein from Col-0 seedlings at times in minutes as indicated following vacuum infiltration with 1 μM flg22 or water (180 min after infiltration). Immunoblots were probed with anti-PAT1 antibodies. Negative control *pat1-1* was loaded for comparison. Coomassie brilliant blue protein loading control is indicated by CBB.

D Anti-GFP immunoblotting of proteins extracted from Col-0/PAT1-GFP seedlings treated over a time course with flg22 (top panel) and Coomassie brilliant blue (CBB)-stained PVDF loading control is shown (bottom panel). No PAT1-GFP was detected in negative control Col-0.

Source data are available online for this figure.

We also find here that PAT1 is an MPK4 substrate and that *pat1* mutants exhibit autoimmunity as does *mpk4*. The connection between MPK4 and PAT1 is further supported by suppression of the *pat1* constitutive defense phenotype by loss-of-function of the SUMM2 R protein (Fig 6). However, SUMM2 deficiency only partially rescues *mpk4* mutants (Zhang *et al*, 2012), thus it is

 © 2015 The Authors

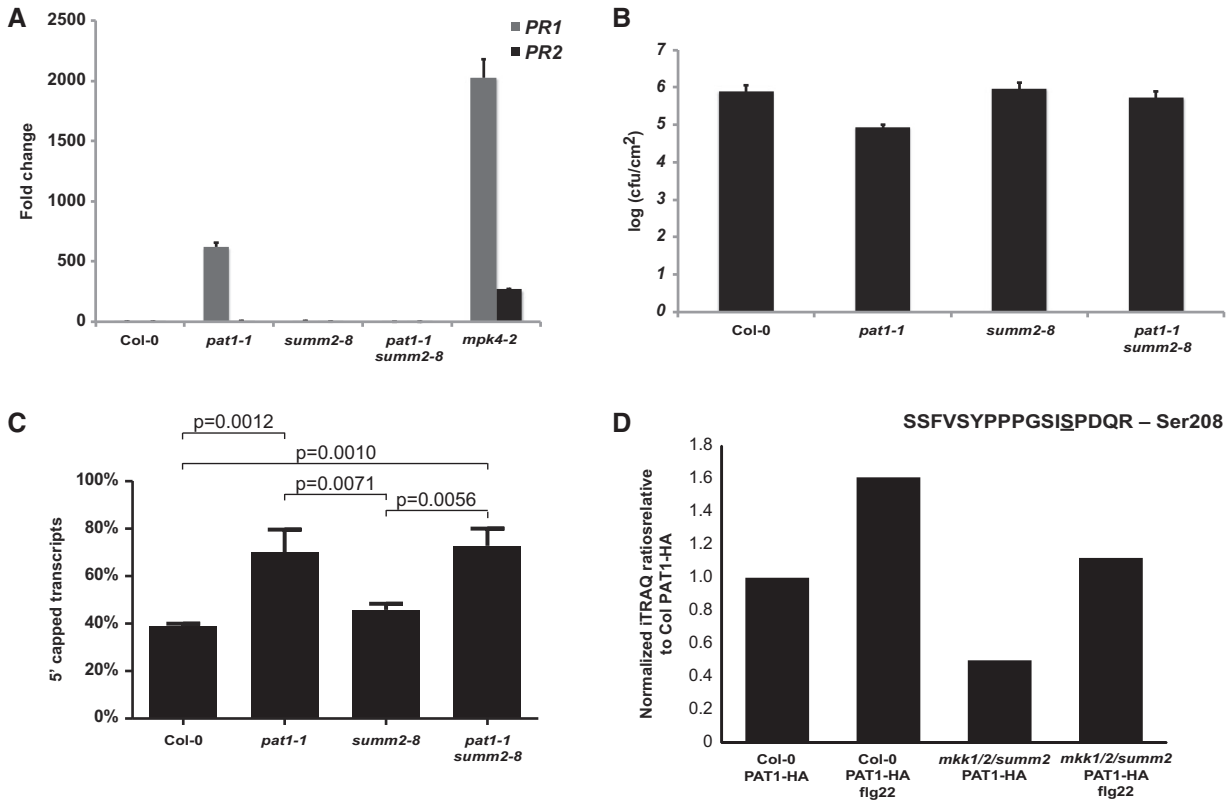

Figure 6. SUMM2 is required for the constitutive defense phenotype of *pat1* mutants.

A Elevated *PR* gene expression in *pat1* mutants is suppressed by *summ2-8*. Four-week-old plants were used for RNA extraction, followed by qRT-PCR. Fold-change in *PR1* (gray bars) and *PR2* (black bars) expression is relative to Col-0, normalized to *UBQ10*. Standard error of the mean is indicated by errors bars (n = 3).

B *pat1* resistance to *P. syringae* pv. *tomato* DC3000 is suppressed by *summ2-8*. Bacteria were syringe-infiltrated and samples taken 3 days post-infiltration. Data are $\log_{10}$-transformed colony-forming units/cm^2 leaf tissue (cfu/cm^2). Standard error of the mean is indicated by errors bars (n = 4).

C 14-day-old seedlings grown on ms plates were used for RNA extraction. Next, 1 μg of RNA from each sample was treated with XRN1 (NEB) or mock treated before RT-qPCR. Data were normalized to *ACT2*, and transcript levels were compared between XRN1 and mock-treated RNA for each genotype. Standard error of the mean is indicated by error bars (n = 4). Statistical significance between the mean values was determined by ANOVA followed by Fisher's LSD test.

D Phosphorylation of the PAT1 peptide SSFVSYPPPGSISPDQR, which include Ser208, in Col-0 and mkk1/1-summ2 before and after flg22 treatment. The phosphorylation stoichiometry is illustrated relative to Col PAT1 without flg22 treatment. The ratios were obtained using quantitative iTRAQ mass spectrometry.

possible that this partial rescue represents a SUMM2 PAT1 branch in the MPK4 pathway. Nevertheless, the *pat1* constitutive defense phenotype is suppressed by *summ2* such that *pat1 summ2* mutants display a wild-type phenotype in response to biotrophic and necrotrophic pathogens (Fig 6; Supplementary Fig S8). Since PAT1 and SUMM2 also interact *in planta* (Fig 7), PAT1, or a PAT1-containing complex, is part of a pathway that includes SUMM2 as well as MPK4. It is therefore possible that PAT1 is under SUMM2 surveillance because it is an effector target with specific functions in immunity. Since *pat1 summ2* mutants are not immunosuppressed, PAT1 and its homologues in *Arabidopsis* may function redundantly during PTI. An alternative explanation is that we simply have not yet tested a pathogen whose infection strategy could reveal a role of PAT1 in immunity.

mRNA decapping is not the only mRNA regulatory pathway characterized by constitutive defense responses. Indeed, mutants of nonsense-mediated decay including *upf3-1*, *upf1-5* and *smg7* mutants display autoimmune phenotypes (Jeong *et al*, 2011; Rayson *et al*, 2012a; Riehs-Kearnan *et al*, 2012; Shi *et al*, 2012). Their phenotypes are also suppressed by mutations in immune regulators such as *eds1* and *pad4* (Rayson *et al*, 2012b; Riehs-Kearnan *et al*, 2012), similar to what we find for *pat1*. This suggests that these components could also be under surveillance and may be suppressed by mutations in specific *R* genes. Recently, it was suggested that nonsense-mediated decay controls turnover of *R* gene mRNAs and cause autoimmunity in *smg7* (Gloggnitzer *et al*, 2014). However, since autoimmunity in *smg7* depends on a specific allele of the R protein RPS6, it is also possible that SMG7 is under surveillance. Most significantly, this suggests that plants have developed complex sensors to monitor the integrity of these pathways, which is consistent with the importance of differential gene expression in response to pathogen perception.

We detected PAT1 phosphorylation by PAMP-activated MPK4, and weakly also by MPK6 *in vitro*. We also identified PAT1 Ser208 and Ser343 as *in planta* phosphorylation sites by mass spectrometry. Since PAT1 phosphorylation was reduced *in vitro* when Ser208 was mutated to Ala, this site may be a key target of MPK4 (Fig 2B). Interestingly, Ser208 is conserved in *Physcomitrella patens* (moss), rice, the *Arabidopsis* PAT1 homologues, and *Xenopus* PATL2, but not in human or yeast PAT1 (Supplementary Fig S10). Although Ser208 corresponds to an SP site in *Xenopus* PATL1/xPAT1b, PATL1

© 2015 The Authors

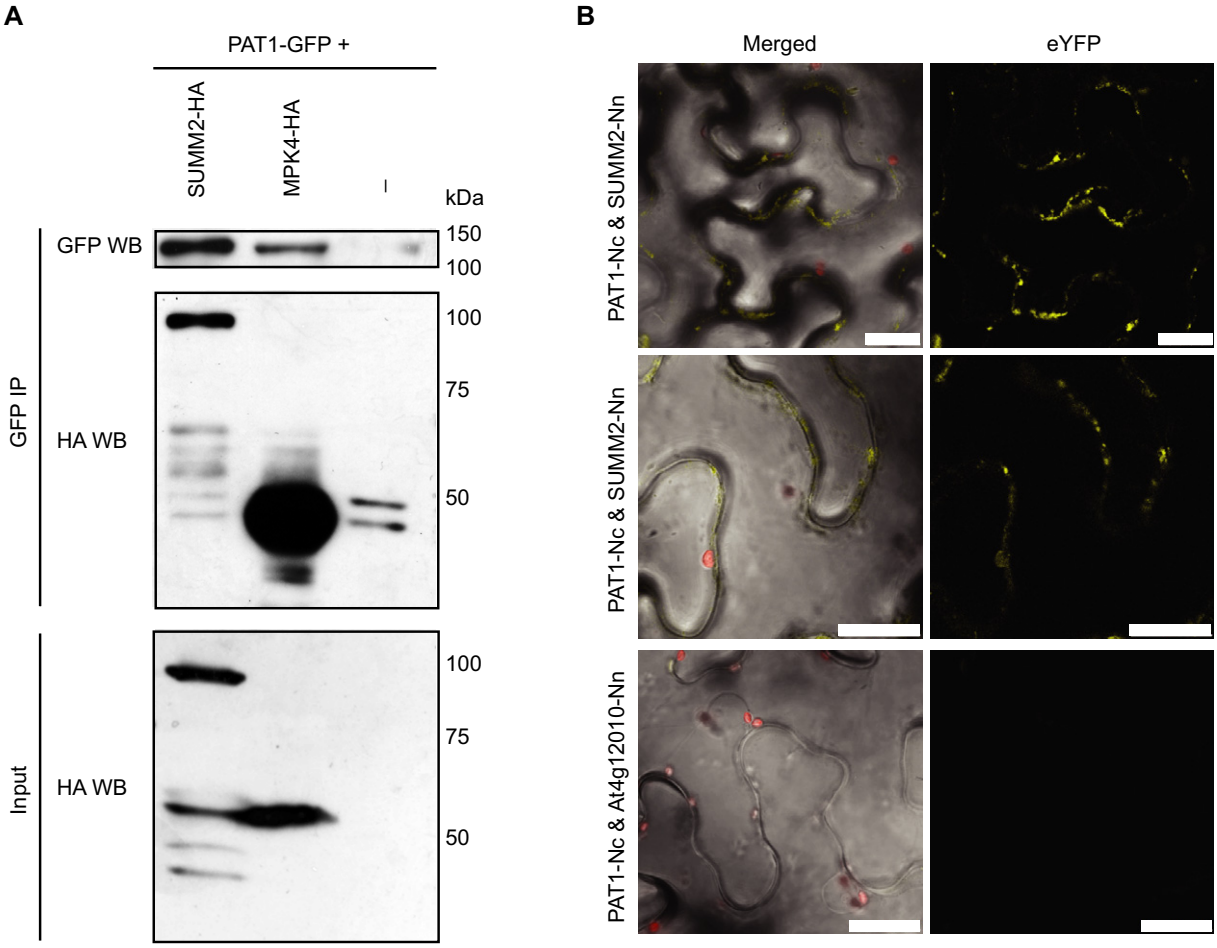

Figure 7. PAT1 is associated with MPK4 and SUMM2 in *N. benthamiana*.

A Proteins were transiently co-expressed (PAT1-GFP + MPK4-HA or SUMM2-HA) in *N. benthamiana* and tissue harvested 2 days post-infiltration. Anti-HA immunoblots of inputs (20 μg each) are shown in the bottom panel. Immunoblots of GFP IPs were probed with anti-HA antibodies, then stripped and probed with anti-GFP antibodies. Molecular weights are shown in kDa on the right.

B Confocal images of yellow fluorescent protein complementation. PAT1-Nc was transiently co-expressed with either SUMM2-Nn or At4g12010 in *N. benthamiana*. Confocal microscopy on leaf disks was conducted 2 days post-infiltration. Merged pictures show overlay of brightfield, chlorophyll and eYFP. The scale bar corresponds to 25 μm.

Source data are available online for this figure.

is known to be phosphorylated on Ser62 by an unknown kinase (Marnef *et al*, 2010). Thus, Ser208 may represent a plant-specific site or mechanism. While Ser208 is conserved in plant PAT1 orthologs, Ser342/3 is not. As Ser342/3 does not correspond to SP sites, they may be phosphorylated by kinases other than MPKs. Furthermore, we detected PAT1 phosphorylation *in planta* irrespective of PAMP treatment.

PAT1 phosphorylation by MPKs has not been shown in any system, although several phosphosites have been identified in human and yeast PAT1 proteins (PhosphoElm, http://phospho.elm.eu.org/ and Phosida http://www.phosida.com/databases). However, other decapping complex members are subject to stress-induced MPK-mediated phosphorylation. For example, human DCP1a is phosphorylated by c-Jun N-terminal kinase in response to stress (Rzeczkowski *et al*, 2011). Similarly, Ste20 phosphorylates yeast DCP2 upon glucose deprivation (Yoon *et al*, 2010). In both cases, phosphorylation seems only to be required for P-body formation and not for general decapping (Yoon *et al*, 2010; Rzeczkowski *et al*, 2011). *Arabidopsis* MPK6 was shown to specifically phosphorylate DCP1 in plants during dehydration stress (Xu & Chua, 2012). Thus, the regulation of mRNA decay machinery by MPKs during stress responses seems to be a key mechanism in plants and other organisms, although exactly how this affects mRNA turnover remains elusive.

Materials and Methods

Plant materials and growth conditions

Arabidopsis thaliana ecotype Columbia (Col-0) was used as a control. Seeds for T-DNA insertion lines were from NASC (Nottingham, UK).

 © 2015 The Authors

The T-DNA lines for At1g79090 (PAT1), both of which have insertions in the last exon, were Salk_040660 (here named *pat1-1*) and WiscDsLox437D04 (*pat1-2*). The T-DNA insertion in At1g12280 (SUMM2) *summ2-8* (SAIL_1152A06), *mkk1/2* (Zhang *et al*, 2012) and *eds1-2* (Parker *et al*, 1996) have been described. Genotyping primers for newly described T-DNA lines are provided in Supplementary Table S1. *Arabidopsis* plants were grown in 9 × 9 cm pots at 22°C with a 8-h photoperiod, or on plates containing Murashige–Skoog (MS) salts medium (Duchefa), 1% sucrose and 1% agar with a 16-h photoperiod.

Cloning and transgenic lines

The genomic PAT1 (At1g79090) DNA sequence (without stop codon), plus 2 kb upstream from the start codon, was amplified from Col-0 genomic DNA and cloned into pENTR-D-TOPO (Invitrogen). The entry clone was recombined into pGWB513, pGWB517 and pGWB504 (Nakagawa *et al*, 2007) to obtain a C-terminal HA, Myc and GFP tags, respectively. The expression clones were transformed into *Agrobacterium tumefaciens* strain GV3101 and transformed into Col-0 plants by floral dipping. Transformants were selected on hygromycin (30 μg/ml) MS agar and survivors tested for protein expression by Western blotting.

The *VCS* promoter region was amplified and inserted into pGEM-T easy and next into the HindIII SalI in pBN:GFP to generate pBNpVCS:GFP. The *VCS* coding region was amplified and cloned into pGEM-T easy next inserted into SalI and KpnI in pBNpVCS:GFP and transformed into *Agrobacterium* LBA4404 and transformed into Col-0 plants by floral dipping. The cDNA of LSM1 (At3g14080) without stop codon was cloned into pENTR-D-TOPO (Invitrogen) and recombined into 35S promoter-containing pGWB505 (Nakagawa *et al*, 2007) to obtain C-terminal GFP-tagged LSM1. Genomic DNA of MPK4 and cDNA of SUMM2 were cloned into pENTR-D-TOPO and recombined into pGWB514 (Nakagawa *et al*, 2007) to obtain C-terminal HA-tagged constructs. The genomic DNA and promoter of DCP1 was cloned into pENTR-D-TOPO and recombined into pGWB513 to obtain C-terminal HA-tagged constructs under the control of the native promoter. Clones were transformed into *A. tumefaciens* strain GV3101 and used for transient expression in *N. benthamiana* or floral dipping in *Arabidopsis*. Genomic PAT1-GFP was transformed into the Col-0 background. DCP1-HA was dipped into the Col-0 background and T3 progeny were crossed with Col-0/PAT1-GFP T4 lines to obtain double transgenic lines. Genomic PAT1-Myc was transformed into Ler *mpk4-1*/MPK4-HA transgenic lines (described in Petersen *et al*, 2000) to obtain double transgenic lines.

The entry clones of PAT1 and SUMM2 were further recombined into pcYGW and pnYGW (Hino *et al*, 2011), respectively, obtaining the N- and C-terminal split YFP tags used for BiFC. At4g12010 clones were obtained by the same procedure. Clones were transformed into *A. tumefaciens* strain GV3101 and used for transient expression in *N. benthamiana.*

Mutagenesis of His_6-PAT1

Site-directed mutagenesis of Ser208 to Ala was accomplished using pET15b-PAT1 as a template for PCR mutagenesis. The primers used were PAT1 S208A F&R (see Supplementary Table S1).

PAT1 protein purification and *in vitro* kinase assays

For *in vitro* experiments, PAT1 protein was purified from *E. coli*. The *PAT1* cDNA was cloned into pET15b (for an N-terminal His fusion) and transformed into *E. coli* BL21 (*pLysS*). Protein expression was induced by overnight treatment with 0.5 mM IPTG at 18°C, added to cells at OD_{600} = 0.6. PAT1 protein was insoluble and thus purified from inclusion bodies using Bugbuster (Novagen). Proteins were solubilized in 6 M urea, 0.7% N-lauroylsarcosine, 100 mM Tris-HCl pH 8 and refolded overnight at 4°C in 0.88 M L-arginine, 55 mM Tris-HCl, 2 mM NaCl, 0.88 mM KCl, protease inhibitors. Protein was then dialyzed against 20 mM Tris-HCl pH 8, 100 mM NaCl using 3,500 MWCO dialysis tubing. Purified protein was concentrated using Centriprep 30K spin columns (Millipore) and then diluted with glycerol to a final concentration of 0.1 mg/ml.

For kinase assays, Col-0 plants were immersed in 200 nM flg22 for 10 min of to activate MAP kinases. MPK3, 4 and 6 were immunoprecipitated from 3 mg total protein extracted from flg22-treated tissue using 2 μg of each of their specific antibodies (Sigma) and 30 μl EZview protein A agarose beads (Sigma). Four microgram of purified myelin basic protein (MBP, Sigma) or 20 μg His_6-PAT1 protein was incubated with washed MPK immunoprecipitates for 60 min at 37°C with 3 μCi γ-ATP in kinase buffer (62.5 μM ATP, 100 mM Tris pH 7.5, 150 mM NaCl, 150 mM $MgCl_2$, 10 mM EGTA, 5 mM DTT, Phosstop inhibitor (Roche)). Kinase reactions were diluted with 4× SDS buffer and boiled for 5 min before loading on 12% SDS-PAGE gels. Following electrophoresis, gels were stained with Coomassie Brilliant Blue and incubated with gel drying buffer, followed by drying on a Bio-Rad gel dryer. Dried gels were exposed to a phosphor screen overnight.

Yeast transformation

Yeast strains *pat1*Δ (BY4742 (YCR077c) *pat1*Δ::*KanMX*) and B4742 were obtained from Euroscarf. PAT1 was cloned from *A. thaliana* Col-0 cDNA into pENTR-D-TOPO and recombined into yeast expression vector pVV215 (C-terminal HA tag, -URA selection; (Van Mullem *et al*, 2003) by Gateway recombination. Yeast *pat1*Δ and B4742 cells were transformed using lithium acetate/polyethylene glycol according to the Clontech Yeast Protocols handbook. Transformed yeast was selected on SD-URA agar plates and re-streaked after 3–4 days onto fresh selection plates. *Pat1*Δ and wild-type-transformed yeast was grown in liquid culture overnight, and protein was extracted from pelleted cells by vortexing with glass beads in 1× SDS extraction buffer. Boiled proteins were subjected to SDS-PAGE and anti-PAT1 immunoblotting. For temperature sensitivity assays, overnight cultures of wild-type, *pat1*Δ and PAT1-expressing transformants were plated on YPAD and grown at 30 and 37°C for 3 days.

Flg22 kinetics

Seedlings were grown on MS agar (Col-0) or MS agar containing 30 μg/ml hygromycin (Col-0/PAT1-GFP) for 5 days before being transferred to MS liquid medium in 24-well plates. After 10 days, seedlings were treated by the addition of flg22 to a final concentration of 100 nM (2 seedlings per well × 3 wells per treatment time

© 2015 The Authors

point). Seedlings were harvested at the indicated times and immediately frozen in liquid nitrogen for later RNA or protein extraction.

Semi-quantitative and qRT-PCR

Total RNA was extracted from seedlings with Tri Reagent (Sigma). RNA samples were treated with DNase Turbo DNA-free (Ambion), quantified with a NanoDrop spectrophotometer (Thermo Scientific) and reverse-transcribed into cDNA with SuperScript III reverse transcriptase (Invitrogen). For semi-quantitative reverse-transcription PCR (RT-PCR), Col-0 seedling cDNA was used as a template for PCR with primers specific for *ACTIN8*, *PAT1*, *PAT1H1* or *PAT1H2* using Sigma Jumpstart REDTaq Readymix. PCR products (20 μl) were separated on 2% (w/v) agarose gels and visualized with ethidium bromide. Brilliant II SybrGreen master mix (Agilent) was used for qPCRs. The *UBQ10* (*At4g05320*) gene was used for normalization. Gene expression of *PR1*, *PR2*, *PAT1* and *SUMM2* was measured by qPCR analysis, normalized to *UBQ10* expression and plotted relative to Col-0 expression level. These experiments were repeated in three independent biological replicates, each with three technical replicates, and representative data are shown. Standard error is represented by error bars on figures, and statistical significance is indicated by letters above error bars. These are derived from one-way ANOVA with Tukey's multiple comparison test (GraphPad Prism).

RNA extraction and RACE PCR

RNA extraction used TRI reagent and 10 μg RNA was used for 5′ RACE according to instructions (First Choice RACE, Ambion). PCR was carried out on 1 μl of products from reverse transcription of capped RNA using DreamTaq polymerase (Fermentas) with 25 cycles. RACE PCR products (10 μl) were separated on 2% (w/v) agarose gels and visualized with ethidium bromide.

Quantification of capped versus uncapped transcripts

Total RNA was extracted from seedlings with NucleoSpin RNA columns (Machery-Nagel). To remove RNA with no 5′ cap structure, 1 μg of total RNA was incubated with 1 unit XRN1 (New England Biolabs) or no enzyme at 37°C for 1 h. Next RNA was reverse-transcribed into cDNA with SuperScript III reverse transcriptase (Invitrogen). *UGT87A2* transcript accumulation was measured by qPCR using SybrGreen master mix (Agilent) and normalized to *ACT2*. Calculating 5′ capped versus uncapped transcripts was done by comparing transcript levels from XRN1 and mock-treated samples for the individual genotypes.

Confocal microscopy

Col-0/PAT1-GFP plants were grown on MS agar containing 30 μg/ml hygromycin for 5 days. Seedlings were placed on glass microscope slides with water, 1% DMSO or 100 nM flg22 for 20 min. For following cycloheximide and DMSO treatment, seedlings were removed from flg22 and placed on new glass microscope slides. Cycloheximide was used at 100 μg/ml in a 1% DMSO dilution, and the control was done with 1% DMSO. Imaging was done using a Leica SP5 inverted microscope.

Infection assays

Pseudomonas syringae pv. *tomato* DC3000 (*Pto* DC3000) strains were grown in overnight culture in Kings B medium supplemented with appropriate antibiotics. Cells were harvested by centrifugation and pellets resuspended in sterile water to $OD_{600} = 0.002$. Bacteria were infiltrated with a needleless 1-mm syringe into four leaves on four plants per genotype and maintained in growth chambers for 3 days. Samples were taken using a cork-borer (6.5 mm) to cut leaf disks from four leaves per plant and four plants per genotype. Leaf disks were ground in water, serially diluted and plated on Kings B with appropriate selection. Plates were incubated at 28°C and colonies counted 2–3 days later. These experiments were repeated in three independent biological replicates, and representative data are shown.

For drop inoculation of *B. cinerea* (strain B05.10), 10 μl of 2.5×10^5 spores/ml in Gamborg B5/2% sucrose (pH 5.6) was placed on the adaxial surface of fully expanded leaves of 4-week-old plants and sampled by harvesting 10–15 leaf disks per genotype were at each time point, namely 0, 2 and 3 days. Data are the average of 3 biological replicates. Disease severity was measured as accumulation of the *B. cinerea CUTINASE A* transcript by qPCR relative to *A. thaliana α-SHAGGY KINASE* (*At5g26751*) (primers are according to Gachon & Saindrenan, 2004).

Transient expression in *Nicotiana benthamiana*

Agrobacterium tumefaciens strains were grown in LB medium supplemented with appropriate antibiotics overnight. Cultures were spun down and resuspended in 10 mM $MgCl_2$ to $OD_{600} = 0.8$. *A. tumefaciens* strains carrying PAT1-GFP and MPK4-HA or SUMM2-HA were mixed 1:1 and syringe-infiltrated into 3-week-old *N. benthamiana* leaves. Samples for protein extraction were harvested 2 days post-infiltration (dpi). *Agrobacterium tumefaciens* strains carrying either PAT1-HA, LSM1-GFP or PAT1-HA + LSM1-GFP were mixed 1:1 and syringe-infiltrated into 3-week-old *N. benthamiana* leaves. Samples for protein extraction were harvested 3 dpi. For BiFC, *A. tumefaciens* strains carrying PAT1 fused to the N-terminal part of YFP and SUMM2 or At4g12010 fused to the C-terminal part were mixed 1:1 and syringe-infiltrated into *N. benthamiana* leaves at an final $OD_{600} = 0.8$. Confocal microscopy on leaf disks was conducted 2 days post-infiltration under a Leica SP5 inverted microscope.

Protein extraction and immunoprecipitation in *Nicotiana benthamiana*

Leaves were ground in liquid nitrogen and extraction buffer [50 mM Tris-HCl pH 7.5; 150 mM NaCl; 10% (v/v) glycerol; 10 mM DTT; 10 mM EDTA; 1% (w/v) PVP; protease inhibitor cocktail (Roche); 0.1% (v/v) IGEPAL CA-630 (Sigma); Phosstop (Roche) added at 2 ml/g tissue powder. Samples were clarified by 20 min centrifugation at 4°C and 13,000 rpm. Supernatants (1.5 ml) were adjusted to 2 mg/ml protein and incubated 2 h at 4°C with 20 μl GFPTrap-A beads (Chromotek) or anti-HA antibodies (2 μg, Santa Cruz) and 30 μl EZview protein A agarose beads (Sigma). Following incubation, beads were washed four times with IP buffer, before adding 30 μl 2× SDS and heating at 95°C for 5 min.

 © 2015 The Authors

Arabidopsis protein extraction and immunoprecipitation for mass spectrometry analysis

Leaves from adult plants were ground in liquid nitrogen and extraction buffer [50 mM Tris-HCl pH 7.5; 150 mM NaCl; 10% (v/v) glycerol; 5 mM DTT; 2 mM EDTA; protease inhibitor cocktail (Roche); 0,1% (v/v) IGEPAL CA-630 (Sigma) and Phosstop (Roche) added at 2 ml/g tissue powder. Samples were clarified by 20 min centrifugation at 4°C 13,000 rpm. Supernatants (45 ml) were adjusted to 3 mg/ml protein and incubated 4 h at 4°C with 50 μl GFPTrap-A beads (Chromotek) or anti-HA antibodies (4 μg, Santa Cruz) and 100 μl EZview protein A agarose beads (Sigma). Following incubation, beads were washed four times with IP buffer before adding 2× SDS and heating to 95°C for 5 min.

SDS-PAGE and immunoblotting

SDS-PAGE gels were prepared with either 8, 10 or 12% cross-linking. Proteins were loaded and gels run at 100–150 V for 1.5 h before electroblotting onto PVDF membrane (GE Healthcare). Membranes were rinsed in TBS and blocked for 1 h in 5% (w/v) non-fat milk in TBS-Tween (0.1% (v/v)). Antibodies were diluted in blocking solution to the following dilutions: anti-GFP (AMS Biotechnology (rabbit) 1:5,000 or Santa Cruz (mouse) 1:1,000), anti-HA 1:1,000 (Santa Cruz). Membranes were incubated with primary antibodies for 1 h to overnight. Membranes were washed 3 × 10 min in TBS-T (0.1%) before 1-h incubation in secondary antibodies, anti-rabbit or anti-mouse-HRP or anti-rabbit or anti-mouse AP conjugate (Promega; 1:5,000). Chemiluminescent substrate (ECL Plus, Pierce) was applied before exposure to film (AGFA CP-BU). For AP-conjugated primary antibodies, membranes were incubated in NBT/BCIP (Roche) until bands were visible. For probing immunoblots with multiple antibodies, stripping was carried out using Restore Western Blot Stripping Buffer (Pierce) for 15–30 min, following by three washes with TBS-Tween.

Antibodies

Polyclonal anti-PAT1 antibodies were generated by immunizing rabbits with synthetic peptides derived from the N-terminus [EQRIPDRTKLYPEPQ] and C-terminus [KRSMLGSQKTEPVLS] of PAT1. Antibodies (final bleed) were affinity-purified against the C-terminal peptide (Eurogentec). Antibody specificity was verified by immunoblotting with plant extracts derived from Col-0 and *pat1-1* tissue. Mouse anti-HA and anti-GFP antibodies were obtained from Santa Cruz. Rabbit anti-GFP antibodies were obtained from AMS Biotechnology. Anti-MPK3, anti-MPK-4 and anti-MPK-6 antibodies were obtained from Sigma. Secondary antibodies were obtained from Promega.

In-gel digestion, TiO_2 chromatography and mass spectrometry

Bands excised from SDS-PAGE were chopped into small pieces and incubated for 1 h in 50 mM TEAB, acetonitrile (50:50) on a shaker at room temperature. After incubation, the sample was centrifuged shortly and the supernatant was discarded. Gel pieces were dried in a vacuum centrifuge for 15 min and subsequently 30 μl of trypsin (10 ng/μl) in 20 mM TEAB pH 7.5 was added to cover the dried gel pieces. The solution was incubated in 4°C for 30 min. After incubation, the trypsin solution was replaced with 30 μl 20 mM TEAB pH 7.5 and the tube was incubated at 37°C overnight. Peptides from the digestion solution after incubation were recovered in a low binding Eppendorf tube (Sorensen Bioscience), and the gel pieces washed with 50% acetonitrile for 15 min to extract more peptides. The washing solution was mixed with the recovered peptides, and the peptide solution was lyophilized. Phosphopeptides were purified by titanium dioxide (TiO_2) chromatography (Larsen *et al*, 2005). Lyophilized peptides were redissolved in loading buffer for TiO_2 chromatography (80% acetonitrile, 5% TFA, 1 M glycolic acid), and 0.3 mg TiO_2 beads (GL Science, Japan) were added to the solution and incubated for 10 min. After incubation, the beads were pelleted by centrifugation and the supernatant was removed. The beads were washed once with 80% acetonitrile, 1% TFA and once with 10% acetonitrile, 0.1% TFA. Phosphopeptides were eluted using 1% ammonium hydroxide and desalted and concentrated prior to LC-MS/MS using a Poros Oligo R3 micro-column (Engholm-Keller *et al*, 2012).

For quantitative phosphopeptide analysis, the tryptic peptide mixtures after in-gel digestion were labeled with iTRAQ 4 plex (according to the manufacturer's protocol) and the samples were mixed prior to TiO_2 enrichment as described above. The non-phosphorylated peptides were concentrated and desalted using a Poros Oligo R3 micro-column (Engholm-Keller *et al*, 2012). The non-phosphorylated peptides were used to normalize the PAT1 protein level.

LC-MS/MS analysis was performed using an EASY-LC system (Proxeon, Thermo Fischer Scientific) coupled to an LTQ-Orbitrap XL mass spectrometer (Thermo Fisher Scientific) as described previously (Engholm-Keller *et al*, 2012). Peptides were separated using a 20 min gradient from 0–34% B-buffer (A-buffer: 0.1% formic acid; B-buffer: 90% acetonitrile, 0.1% formic acid). The data-dependent analysis was performed using one MS full scan in the area 300–1,800 Da performed in the Orbitrap with 60,000 in resolution, followed by the five most intense ions selected for MSMS (collision induced dissociation) performed in the linear ion trap.

Raw data from the LTQ-Orbitrap-XL were processed using the Proteome Discoverer (PD) program (Thermo Fisher Scientific, Bremen, Germany). The data were searched against the *Arabidopsis* database (33,596 sequences; 13,487,687 residues) using the Mascot 2.2 version database. The parameters for the database search were as follows: Enzyme—trypsin; missed cleavages—2; MS mass accuracy—10 ppm; MSMS mass accuracy—0.8 Da; Variable modifications—Phosphorylation (S, T, Y), Oxidation (met), Propionamide (C). The identified peptides were filtered for 1% false discovery rate using the 'Fixed Value PSM Validator' in PD. All identified phosphopeptides were manually validated. For iTRAQ-labeled phosphopeptides, the PD quantitation node was used and the data were normalized based on the non-phosphorylated peptides.

Supplementary information for this article is available online: http://emboj.embopress.org

Acknowledgements

We thank Yuelin Zhang for providing *summ2-8* and *mkk1/2 summ2-8* seeds. This work was supported by the Danish Research Council for independent Research, Natural Sciences Grant #10-084139 (M.P.) & Postdoctoral Fellowship

© 2015 The Authors

#11-116368 (M.E.R.) & Technology and Production Sciences #11-106302. KP was supported by an EMBO Long-Term Fellowship and a Marie Curie International Incoming Fellowship. We thank Suksawad Vonvisuttikun for technical help and Dr. Tsuyoshi Nakagawa (Shimane University) for providing Gateway binary pGWB vectors. All confocal work was done at Center for Advanced Bioimaging. MRL was supported by the Lundbeck Foundation (Junior Group Leader Fellowship).

Author contributions

MER, MWR, KP, JM and MP conceived and designed the experiments. MER, MWR KP, SL, MRL, JG, AMR, LS, WZ and GB performed experiments. MER, MWR, JM and MP analyzed the data. MER, MWR, JM and MP wrote the manuscript.

Conflict of interest

The authors declare that they have no conflicts of interest.

References

Andreasson E, Jenkins T, Brodersen P, Thorgrimsen S, Petersen NH, Zhu S, Qiu J-L, Micheelsen P, Rocher A, Petersen M, Newman M-A, Nielsen HB, Hirt H, Somssich IE, Mattsson O, Mundy J (2005) The MAP kinase substrate MKS1 is a regulator of plant defense responses. *EMBO J* 24: 2579 – 2589

Andreasson E, Ellis B (2010) Convergence and specificity in the *Arabidopsis* MAPK nexus. *Trends Plant Sci* 15: 106 – 113

Asai T, Tena G, Plotnikova J, Willmann MR, Chiu WL, Gómez-Gómez L, Boller T, Ausubel FM, Sheen J (2002) MAP kinase signalling cascade in *Arabidopsis* innate immunity. *Nature* 415: 977 – 983

Balagopal V, Parker R (2009) Polysomes, P bodies and stress granules: states and fates of eukaryotic mRNAs. *Curr Opin Cell Biol* 21: 403 – 408

Barišić-Jäger E, Kręcioch I, Hosiner S, Antic S, Dorner S (2013) HPat a decapping activator interacting with the miRNA effector complex. *PLoS One* 8: e71860

Bethke G, Unthan T, Uhrig JF, Poeschl Y, Gust AA, Scheel D, Lee J (2009) Flg22 regulates the release of an ethylene response factor substrate from MAP kinase 6 in *Arabidopsis thaliana* via ethylene signaling. *PNAS* 106: 674

Bethke G, Pecher P, Eschen-Lippold L, Tsuda K, Katagiri F, Glazebrook J, Scheel D, Lee J (2012) Activation of the *Arabidopsis thaliana* mitogen-activated protein kinase MPK11 by the flagellin-derived elicitor peptide, flg22. *Mol Plant Microbe Interact* 25: 471 – 480

Blewett NH, Goldstrohm AC (2012) A eukaryotic translation initiation factor 4E-binding protein promotes mRNA decapping and is required for PUF repression. *Mol Cell Biol* 32: 4181 – 4194

Boag PR, Atalay A, Robida S, Reinke V, Blackwell TK (2008) Protection of specific maternal messenger RNAs by the P body protein CGH-1 (Dhh1/RCK) during *Caenorhabditis elegans* oogenesis. *J Cell Biol* 182: 543 – 557

Boller T, Felix G (2009) A renaissance of elicitors: perception of microbe-associated molecular patterns and danger signals by pattern-recognition receptors. *Annu Rev Plant Biol* 60: 379 – 406

Bonnerot C, Boeck R, Lapeyre B (2000) The two proteins Pat1p (Mrt1p) and Spb8p interact *in vivo*, are required for mRNA decay, and are functionally linked to Pab1p. *Mol Cell Biol* 20: 5939 – 5946

Bouveret E, Rigaut G, Shevchenko A, Wilm M, Seraphin B (2000) A Sm-like protein complex that participates in mRNA degradation. *EMBO J* 19: 1661 – 1671

Brader G, Djamei A, Teige M, Palva ET, Hirt H (2007) The MAP kinase kinase MKK2 affects disease resistance in *Arabidopsis*. *Mol Plant Microbe Interact* 20: 589 – 596

Brengues M (2005) Movement of eukaryotic mRNAs between polysomes and cytoplasmic processing bodies. *Science* 310: 486 – 489

Brodersen P, Petersen M, Nielsen H, Zhu S, Newman M-A, Shokat KM, Rietz S, Parker J, Mundy J (2006) *Arabidopsis* MAP kinase 4 regulates salicylic acid- and jasmonic acid/ethylene-dependent responses via EDS1 and PAD4. *Plant J* 47: 532 – 546

Brodersen P, Sakcarelidze-Achard L, Bruun-Rasmussen M, Dunoyer P, Yamamoto YY, Sieburth L, Voinnet O (2008) Widespread translational inhibition by plant miRNAs and siRNAs. *Science* 320: 1185 – 1190

Buchan JR, Yoon J-H, Parker R (2011) Stress-specific composition, assembly and kinetics of stress granules in *Saccharomyces cerevisiae*. *J Cell Sci* 124: 228 – 239

Chinchilla D, Bauer Z, Regenass M, Boller T, Felix G (2006) The *Arabidopsis* receptor kinase FLS2 binds flg22 and determines the specificity of flagellin perception. *Plant Cell* 18: 465 – 476

Chisholm ST, Coaker G, Day B, Staskawicz BJ (2006) Host-microbe interactions: shaping the evolution of the plant immune response. *Cell* 124: 803 – 814

Coller J, Parker R (2005) General translational repression by activators of mRNA decapping. *Cell* 122: 875 – 886

Deyholos MK, Cavaness GF, Hall B, King E, Punwani J, van Norman J, Sieburth L (2003) VARICOSE, a WD-domain protein, is required for leaf blade development. *Development* 130: 6577 – 6588

Droillard M-J, Boudsocq M, Barbier-Brygoo H, Laurière C (2004) Involvement of MPK4 in osmotic stress response pathways in cell suspensions and plantlets of *Arabidopsis thaliana*: activation by hypoosmolarity and negative role in hyperosmolarity tolerance. *FEBS Lett* 574: 42 – 48

Engholm-Keller K, Birck P, Størling J, Pociot F, Mandrup-Poulsen T, Larsen MR (2012) TiSH–a robust and sensitive global phosphoproteomics strategy employing a combination of TiO2, SIMAC, and HILIC. *J Proteomics* 75: 5749 – 5761

Gachon C, Saindrenan P (2004) Real-time PCR monitoring of fungal development in Arabidopsis thaliana infected by *Alternaria brassicicola* and *Botrytis cinerea*. *Plant Physiol Biochem* 42: 367 – 371

Gao M, Liu J, Bi D, Zhang Z, Cheng F, Chen S, Zhang Y (2008) MEKK1, MKK1/MKK2 and MPK4 function together in a mitogen-activated protein kinase cascade to regulate innate immunity in plants. *Cell Res* 18: 1190 – 1198

Garneau NL, Wilusz J, Wilusz CJ (2007) The highways and byways of mRNA decay. *Nat Rev Mol Cell Biol* 8: 113 – 126

Glazebrook J (2005) Contrasting mechanisms of defense against biotrophic and necrotrophic pathogens. *Annu Rev Phytopathol* 43: 205 – 227

Gloggnitzer J, Akimcheva S, Srinivasan A, Kusenda B, Riehs N, Stampfl H, Bautor J, Dekrout B, Jonak C, Jimenez-Gomez JM, Parker JE, Riha K (2014) Nonsense-mediated mRNA decay modulates immune receptor levels to regulate plant antibacterial defense. *Cell Host Microbe* 16: 376 – 390

Goeres D, Van Norman JM, Zhang W, Fauver NA, Spencer ML, Sieburth L (2007) Components of the *Arabidopsis* mRNA decapping complex are required for early seedling development. *Plant Cell* 19: 1549 – 1564

Golisz A, Sikorski PJ, Kruszka K, Kufel J (2013) *Arabidopsis thaliana* LSM proteins function in mRNA splicing and degradation. *Nucleic Acids Res* 41: 6232 – 6249

Gomez-Gomez L, Bauer Z, Boller T (2001) Both the extracellular leucine-rich repeat domain and the kinase activity of FLS2 are required for flagellin binding and signaling in *Arabidopsis*. *Plant Cell* 13: 1155 – 1163

 © 2015 The Authors

Gregory BD, Lister R, OMalley R, Urich MA, Tonti-Phillipini J, Chen H, Millar AH, Ecker JR (2008) A link between RNA metabolism and silencing affecting *Arabidopsis* development. *Dev Cell* 14: 854 – 866

Grigg SP, Canales C, Hay A, Tsiantis M (2005) SERRATE coordinates shoot meristem function and leaf axial patterning in *Arabidopsis*. *Nature* 437: 1022 – 1026

Haas G, Braun JE, Tritschler F, Nishihara T, Izaurralde E (2010) HPat provides a link between deadenylation and decapping in metazoa. *J Cell Biol* 189: 289 – 302

Hatfield L, Beelman CA, Stevens A, Parker R (1996) Mutations in trans-acting factors affecting mRNA decapping in Saccharomyces cerevisiae. *Mol Cell Biol* 16: 5830 – 5838

Hino T, Tanaka Y, Kawamukai M, Nishimura K, Mano S, Nakagawa T (2011) Two Sec13p homologs, AtSec13A and AtSec13B, redundantly contribute to the formation of COPII transport vesicles in *Arabidopsis thaliana*. *Biosci Biotechnol Biochem* 75: 1848 – 1852

Ichimura K, Casais C, Peck SC, Shinozaki K, Shirasu K (2006) MEKK1 is required for MPK4 activation and regulates tissue-specific and temperature-dependent cell death in *Arabidopsis*. *J Biol Chem* 281: 36969 – 36976

Jeong H-J, Kim YJ, Kim SH, Kim Y-H, Lee I-J, Kim YK (2011) Nonsense-mediated mRNA decay factors, UPF1 and UPF3, contribute to plant defense. *Plant Cell Physiol* 52: 2147 – 2156

Jiao X, Xiang S, Oh C, Martin CE, Tong L, Kiledjan M (2010) Identification of a quality-control mechanism for mRNA 5′-end capping. *Nature* 467: 608 – 611

Jones JDG, Dangl JL (2006) The plant immune system. *Nature* 444: 323 – 329

Kulkarni M, Ozgur S, Stoecklin G (2010) On track with P-bodies. *Biochem Soc Trans* 38: 242 – 251

Larsen MR, Thingholm TE, Jensen ON, Roepstorff P, Jørgensen TJD (2005) Highly selective enrichment of phosphorylated peptides from peptide mixtures using titanium dioxide microcolumns. *Mol Cell Proteomics* 4: 873 – 886

Li S, Liu L, Zhuang X, Yu Y, Liu X, Cui X, Ji L, Pan Z, Cao X, Mo B, Zhang F, Raikhel N, Jiang L, Chen X (2013) MicroRNAs inhibit the translation of target mRNAs on the endoplasmic reticulum in *Arabidopsis*. *Cell* 153: 562 – 574

Marnef A, Maldonado M, Buguaut A, Balasubramanian S, Kress M, Weil D, Standart N (2010) Distinct functions of maternal and somatic Pat1 protein paralogs. *RNA* 16: 2094 – 2107

Marnef A, Standart N (2010) Pat1 proteins: a life in translation, translation repression and mRNA decay. *Biochem Soc Trans* 38: 1602 – 1607

Mészáros T, Helfer A, Hatzimasoura E, Magyar Z, Serazetdinova L, Rios G, Bardóczy V, Teige M, Koncz C, Peck S, Bögre L (2006) The *Arabidopsis* MAP kinase kinase MKK1 participates in defence responses to the bacterial elicitor flagellin. *Plant J* 48: 485 – 498

Morel JB (2002) Fertile hypomorphic *ARGONAUTE* (*ago1*) mutants impaired in post-transcriptional gene silencing and virus resistance. *Plant Cell* 14: 629 – 639

Motomura K, Le QT, Kumakura N, Fukaya T, Takeda A, Watanabe Y (2012) The role of decapping proteins in the miRNA accumulation in *Arabidopsis thaliana*. *RNA Biol* 9: 644 – 652

Munchel SE, Shultzaberger RK, Takizawa N, Weis K (2011) Dynamic profiling of mRNA turnover reveals gene-specific and system-wide regulation of mRNA decay. *Mol Biol Cell* 22: 2787 – 2795

Nakagawa T, Kurose T, Hino T, Kawamukai M, Niwa Y, Toyooka K, Matsuoka K, Jinbo T, Kimura T (2007) Development of series of gateway binary vectors, pGWBs, for realizing efficient construction of fusion genes for plant transformation. *J Biosci Bioeng* 104: 34 – 41

Nikovics K, Blein T, Peaucelle A, Ishida T, Morin H, Aida M, Laufs P (2006) The balance between the MIR164A and CUC2 genes controls leaf margin serration in Arabidopsis. *Plant Cell* 18: 2929 – 2945

Nissan T, Rajyaguru P, She M, Song H, Parker R (2010) Decapping activators in *Saccharomyces cerevisiae* act by multiple mechanisms. *Mol Cell* 39: 773 – 783

Olmedo G, Guo H, Gregory BD, Nourizadeh SD, Aguilar-Henonin L, Li H, An F, Guzman P, Ecker JR (2006) ETHYLENE-INSENSITIVE5 encodes a 5 '-> 3 ' exoribonuclease required for regulation of the EIN3-targeting F-box proteins EBF1/2. *PNAS* 103: 13286 – 13293

Ozgur S, Chekulaeva M, Stoecklin G (2010) Human Pat1b connects deadenylation with mRNA decapping and controls the assembly of processing bodies. *Mol Cell Biol* 30: 4308 – 4323

Park S-H, Chung PJ, Juntawong P, Bailey-Serres J, Kim YS, Jung H, Bang SW, Kim Y-K, Do Choi Y, Kim J-K (2012) Posttranscriptional control of photosynthetic mRNA decay under stress conditions requires 3′ and 5′ untranslated regions and correlates with differential polysome association in rice. *Plant Physiol* 159: 1111 – 1124

Parker JE, Holub EB, Frost LN, Falk A, Gunn ND, Daniels MJ (1996) Characterization of *eds1*, a mutation in *Arabidopsis* suppressing resistance to *Peronospora parasitica* specified by several different *RPP* genes. *Plant Cell* 8: 2033 – 2046

Parker R, Sheth U (2007) P bodies and the control of mRNA translation and degradation. *Mol Cell* 25: 635 – 646

Pearson G, Robinson F, Gibson TB, Xu BE, Karandikar M, Berman K, Cobb MH (2001) Mitogen-activated protein (MAP) kinase pathways: regulation and physiological functions. *Endocr Rev* 22: 153 – 183

Perea-Resa C, Hernández-Verdeja T, López-Cobollo R, del Mar Castellano M, Salinas J (2012) LSM proteins provide accurate splicing and decay of selected transcripts to ensure normal *Arabidopsis* development. *Plant Cell* 24: 4930 – 4947

Petersen M, Brodersen P, Naested H, Andreasson E, Lindhart U, Johansen B, Nielsen HB, Lacy M, Austin MJ, Parker JE, Sharma SB, Klessig DF, Martienssen R, Mattsson O, Jensen AB, Mundy J (2000) *Arabidopsis* MAP kinase 4 negatively regulates systemic acquired resistance. *Cell* 103: 1111 – 1120

Pitzschke A, Schikora A, Hirt H (2009) MAPK cascade signalling networks in plant defence. *Curr Opin Plant Biol* 12: 421 – 426

Potuschak T, Vansiri A, Binder BM, Vierstra RD, Genschik P (2006) The exoribonuclease XRN4 is a component of the ethylene response pathway in *Arabidopsis*. *Plant Cell* 18: 3047 – 3057

Qiu J-L, Fiil BK, Petersen K, Nielsen HB, Botanga CJ, Thorgrimsen S, Palma K, Suarez-Rodriguez MC, Sandbech-Clausen S, Lichota J, Brodersen P, Grasser KD, Mattsson O, Glazebrook J, Mundy J, Petersen M (2008a) *Arabidopsis* MAP kinase 4 regulates gene expression through transcription factor release in the nucleus. *EMBO J* 27: 2214 – 2221

Qiu J-L, Zhou L, Yun B-W, Nielsen HB, Fiil BK, Petersen K, MacKinlay J, Loake GJ, Mundy J, Morris PC (2008b) *Arabidopsis* mitogen-activated protein kinase kinases MKK1 and MKK2 have overlapping functions in defense signaling mediated by MEKK1, MPK4, and MKS1. *Plant Physiol* 148: 212 – 222

Rasmussen MW, Roux M, Petersen M, Mundy J (2012) MAP kinase cascades in *Arabidopsis* innate immunity. *Front Plant Sci* 3: 169

Ravet K, Reyt G, Arnaud N, Krouk G, Djouani E, Boucherez J, Briat J, Gaymard F (2012) Iron and ROS control of the DownSTream mRNA decay pathway is essential for plant fitness. *EMBO J* 31: 175 – 186

Rayson S, Arciga-Reyes L, Wooton L, de Torres Zabala M, Truman W, Grant M, Davies B (2012a) A role for nonsense-mediated mRNA decay in plants: pathogen responses are induced in *Arabidopsis thaliana* NMD mutants. *PLoS One* 7: e31917

© 2015 The Authors

Rayson S, Ashworth M, de Torres Zabala M, Grant M, Davies B (2012b) The salicylic acid dependent and independent effects of NMD in plants. *Plant Signal Behav* 7: 1434 – 1437

Riehs-Kearnan N, Gloggnitzer J, Dekrout B, Jonak C, Riha K (2012) Aberrant growth and lethality of *Arabidopsis* deficient in nonsense-mediated RNA decay factors is caused by autoimmune-like response. *Nucleic Acids Res* 40: 5615 – 5624

Rodriguez-Cousino N, Lill R, Neupert W, Court D (1995) Identification and initial characterization of the cytosolic protein Ycr77p. *Yeast* 11: 581 – 585

Rymarquis LA, Souret FF, Green PJ (2011) Evidence that XRN4, an *Arabidopsis* homolog of exoribonuclease XRN1, preferentially impacts transcripts with certain sequences or in particular functional categories. *RNA* 17: 501 – 511

Rzeczkowski K, Beuerlein K, Müller H, Dittrich-Breiholz O, Schneider H, Kettner-Buhrow D, Holtmann H, Kracht M (2011) c-Jun N-terminal kinase phosphorylates DCP1a to control formation of P bodies. *J Cell Biol* 194: 581 – 596

Salgado-Garrido J, Bragado-Nilsson E, Kandels-Lewis S, Seraphin B (1999) Sm and Sm-like proteins assemble in two related complexes of deep evolutionary origin. *EMBO J* 18: 3451 – 3462

Scheller N, Resa-Infante P, la Luna de S, Galao RP, Albrecht M, Kaestner L, Lipp P, Lengauer T, Meyerhans A, Díez J (2007) Identification of PatL1, a human homolog to yeast P body component Pat1. *Biochim Biophys Acta* 1773: 1786 – 1792.

Shi C, Baldwin I, Wu J (2012) *Arabidopsis* plants having defects in nonsense-mediated mRNA decay factors UPF1, UPF2, and UPF3 show photoperiod-dependent phenotypes in development and stress responses. *J Integr Plant Biol* 54: 99 – 114

Suarez-Rodriguez MC, Adams-Phillips L, Liu Y, Wang H, Su S-H, Jester PJ, Zhang S, Bent AF, Krysan PJ (2007) MEKK1 is required for flg22-induced MPK4 activation in *Arabidopsis* plants. *Plant Physiol* 143: 661 – 669

Teige M, Scheikl E, Eulgem T, Doczi F, Ichimura K, Shinozaki K, Dangl JL, Hirt H (2004) The MKK2 pathway mediates cold and salt stress signaling in *Arabidopsis*. *Mol Cell* 15: 141 – 152

Tharun S, He WH, Mayes AE, Lennertz P, Beggs JD, Parker R (2000) Yeast Sm-like proteins function in mRNA decapping and decay. *Nature* 404: 515 – 518

Tharun S, Parker R (2001) Targeting an mRNA for decapping: displacement of translation factors and association of the Lsm1p-7p complex on deadenylated yeast mRNAs. *Mol Cell* 8: 1075 – 1083

Tharun S, Muhlrad D, Chowdhury A, Parker R (2005) Mutations in the *Saccharomyces cerevisiae LSM1* gene that affect mRNA decapping and 3′ end protection. *Genetics* 170: 33 – 46

Tharun S (2009) Lsm1-7-Pat1 complex. *RNA Biol* 6: 228 – 232

Thomas M, Loschi M, Desbats M, Boccaccio G (2011) RNA granules: the good, the bad and the ugly. *Cell Signal* 23: 324 – 334

Totaro A, Renzi F, La Fata G, Mattioli C, Raabe M, Urlaub H, Achsel T (2011) The human Pat1b protein: a novel mRNA deadenylation factor identified by a new immunoprecipitation technique. *Nucleic Acids Res* 39: 635 – 647

Ubersax JA, Ferrell JE Jr (2007) Mechanisms of specificity in protein phosphorylation. *Nat Rev Mol Cell Biol* 8: 530 – 541

Van Mullem V, Wery M, De Bolle X, Vandenhaute J (2003) Construction of a set of *Saccharomyces cerevisiae* vectors designed for recombinational cloning. *Yeast* 20: 739 – 746

Vogel F, Hofius D, Paulus KE, Jungkunz I, Sonnewald U (2011) The second face of a known player: *Arabidopsis* silencing suppressor AtXRN4 acts organ-specifically. *New Phytol* 189: 484 – 493

Wang X, Watt P, Louis E, Borts RH, Hickson I (1996) Pat1: a topoisomerase II-associated protein required for faithful chromosome transmission in *Saccharomyces cerevisiae*. *Nucleic Acids Res* 24: 4791 – 4797

Weber C, Nover L, Fauth M (2008) Plant stress granules and mRNA processing bodies are distinct from heat stress granules. *Plant J* 56: 517 – 530

Xu J, Yang J-Y, Niu Q-W, Chua N-H (2006) *Arabidopsis* DCP2, DCP1, and VARICOSE form a decapping complex required for postembryonic development. *Plant Cell* 18: 3386 – 3398

Xu J, Chua NH (2009) *Arabidopsis* decapping 5 is required for mRNA decapping, P-Body formation, and translational repression during postembryonic development. *Plant Cell* 21: 3270 – 3279

Xu J, Chua N-H (2011) Processing bodies and plant development. *Curr Opin Plant Biol* 14: 88 – 93

Xu J, Chua NH (2012) Dehydration stress activates Arabidopsis MPK6 to signal DCP1 phosphorylation. *EMBO J* 31: 1975 – 1984

Yang L, Wu G, Poethig RS (2012) Mutations in the GW-repeat protein SUO reveal a developmental function for microRNA-mediated translational repression in Arabidopsis. *PNAS* 109: 315 – 320

Yoon J-H, Choi E-J, Parker R (2010) Dcp2 phosphorylation by Ste20 modulates stress granule assembly and mRNA decay in *Saccharomyces cerevisiae*. *J Cell Biol* 189: 813 – 827

Zhang J, Shao F, Li Y, Cui H, Chen L, Li H, Zou Y, Long C, Lan L, Chai J, Chai J, Chen S, Tang X, Zhou J-M (2007) A *Pseudomonas syringae* effector inactivates MAPKs to suppress PAMP-induced immunity in plants. *Cell Host Microbe* 1: 175 – 185

Zhang Z, Wu Y, Gao M, Zhang J, Kong Q, Liu Y, Ba H, Zhou J, Zhang Y (2012) Disruption of PAMP-induced MAP kinase cascade by a *Pseudomonas syringae* effector activates plant immunity mediated by the NB-LRR protein SUMM2. *Cell Host Microbe* 11: 253 – 263

Zipfel C (2009) Early molecular events in PAMP-triggered immunity. *Curr Opin Plant Biol* 12: 414 – 420

 © 2015 The Authors